

1 **Role of a key microphysical factor in mixed-phase stratocumulus clouds and their**
 2 **interactions with aerosols**

3
 4 Seoung Soo Lee^{1,2,3}, Chang-Hoon Jung⁴, Jinho Choi⁵, Young Jun Yoon⁶, Junshik Um^{5,7},
 5 Youtong Zheng⁸, Jianping Guo⁹, Manguttathil. G. Manoj¹⁰, Sang-Keun Song¹¹

6
 7 ¹Science and Technology Corporation, Hampton, Virginia
 8 ²Earth System Science Interdisciplinary Center, University of Maryland, College Park,
 9 Maryland, USA
 10 ³Research Center for Climate Sciences, Pusan National University, Busan, Republic of
 11 Korea
 12 ⁴Department of Health Management, Kyungin Women's University, Incheon, Republic of
 13 Korea
 14 ⁵Department of Atmospheric Sciences, Pusan National University, Busan, Republic of
 15 Korea
 16 ⁶Korea Polar Research Institute, Incheon, Republic of Korea
 17 ⁷Institute of Environmental Studies, Pusan National University, Busan, Republic of Korea
 18 ⁸Department of Earth and Atmospheric Sciences, University of Houston, Houston, Texas,
 19 USA
 20 ⁹State Key Laboratory of Severe Weather, Chinese Academy of Meteorological Sciences,
 21 Beijing 100081, China
 22 ¹⁰Advanced Centre for Atmospheric Radar Research, Cochin University of Science and
 23 Technology, Kerala, India

Deleted: Examination of

Deleted: varying

Deleted: in terms of their properties, ice processes and aerosol-cloud interactions between polar and midlatitude cases: An attempt to propose a microphysical factor to explain the variation[¶]

30 ¹¹Department of Earth and Marine Sciences, Jeju National University, Jeju, Republic of
31 Korea

32

33

34

35

36

37

38

39

40

41

42

43

44

45

46

47

48

49

50

51

52 Corresponding author: Seoung Soo Lee, Chang-Hoon Jung and Sang-Keun Song

53 Office: (303) 497-6615

54 Cell: (609) 375-6685

55 Fax: (303) 497-5318

56 E-mail: cumulss@gmail.com, slee1247@umd.edu

57

58

59

60 Abstract

61

62 This study examines the ratio of ice crystal number concentration (ICNC) to cloud droplet
63 number concentration (CDNC), which is ICNC/CDNC, in mixed-phase stratocumulus
64 clouds. This examination is performed using a large-eddy simulation (LES) framework and
65 one of efforts toward a more general understanding of mechanisms controlling cloud
66 development, aerosol-cloud interactions and impacts of ice processes on them in mixed-
67 phase stratocumulus clouds. For the examination, this study compares a case of polar
68 mixed-phase stratocumulus clouds to that of midlatitude mixed-phase stratocumulus
69 clouds with weak precipitation. It is found that ICNC/CDNC plays a critical role in making
70 differences in cloud development with respect to the relative proportion of liquid and ice
71 mass between the cases by affecting in-cloud latent-heat processes. Note that this
72 proportion has an important implication for cloud radiative properties and thus climate. It
73 is also found that ICNC/CDNC plays a critical role in making differences in interactions
74 between clouds and aerosols and impacts of ice processes on clouds and their interactions
75 with aerosols between the cases by affecting in-cloud latent-heat processes. Findings of
76 this study suggest that ICNC/CDNC can be a simplified general factor that contributes to
77 a more general understanding and parameterizations of mixed-phase clouds, their
78 interactions with aerosols and roles of ice processes in them.

79

80

81

82

83

84

85

86

87

88

89

90

91 1. Introduction

92

93 Stratiform clouds (e.g., stratus and stratocumulus clouds) have significant impacts on
94 climate (Warren et al. 1986; Stephens and Greenwald 1991; Hartmann et al. 1992; Hahn
95 and Warren 2007; Wood, 2012; Dione et al., 2019; Zheng et al., 2021). Since
96 industrialization, aerosol concentrations have increased and this has had impacts on
97 stratiform clouds and climate (Twomey, 1974; Albrecht, 1989; Ackerman et al., 2004).
98 However, our level of understanding of these clouds and impacts has been low and this has
99 caused the highest uncertainty in the prediction of future climate (Ramaswamy et al., 2001;
100 Forster et al., 2007; Knippertz et al., 2011; Hannak et al., 2017). Stratiform clouds can be
101 classified into warm and mixed-phase clouds. Mixed-phase stratiform clouds involve ice
102 processes and frequently form in midlatitude and polar regions. When mixed-phase clouds
103 are associated with convective clouds, they can form even in the tropical region. Most
104 previous studies have focused on warm clouds and their interactions with aerosols, whereas
105 the mixed-phase stratiform clouds and their interactions with aerosols are poorly
106 understood mainly due to the more complex ice processes. Hence, mixed-phase stratiform
107 clouds and their interactions with aerosols account for the uncertainty more than warm
108 clouds and their interactions with aerosols (Ramaswamy et al., 2001; Forster et al., 2007;
109 Wood, 2012; IPCC, 2021; Li et al., 2022).

110 The relative proportion of liquid mass, which can be represented by liquid-water
111 content (LWC) or liquid-water path (LWP), and ice mass, which can be represented by ice-
112 water content (IWC) or ice-water path (IWP), in mixed-phase stratiform clouds plays a
113 critical role in cloud radiative properties and thus their climate feedbacks (Tsushima et
114 al., 2006; Choi et al., 2010 and 2014; Gettelman et al., 2012; Zhang et al., 2019). The
115 relative proportion is defined to be IWC (IWP) over LWC (LWP) or IWC/LWC
116 (IWP/LWP) in this study. Motivated by this and the above-mentioned uncertainty, this
117 study aims to improve our understanding of mixed-phase stratiform clouds and their
118 interactions with aerosols with the emphasis on ice processes and IWC/LWC (or
119 IWP/LWP).

120 Lee et al. (2021) have investigated mixed-phase stratocumulus clouds in a midlatitude
121 region and found that microphysical latent-heat processes are more important in the

Deleted: stratiform

123 development of mixed-phase stratiform clouds and their interactions with aerosols than
 124 entrainment and sedimentation processes. Lee et al. (2021) have found that a microphysical
 125 factor, the ratio of ice crystal number concentration (ICNC) to cloud droplet number
 126 concentration (CDNC) or ICNC/CDNC, play an important role in latent processes, the
 127 development of mixed-phase stratiform clouds and their interactions with aerosols. In
 128 particular, Lee et al. (2021) have found that IWC/LWC or IWP/LWP is strongly affected
 129 by ICNC/CDNC. ~~This is because water vapor deposits on the surface of ice crystals, while~~
 130 ~~it condenses on droplets. As a result, ice crystals act as sources of deposition and droplets~~
 131 ~~act as sources of condensation. Consequently, ice crystals act as sources of IWC (or IWP)~~
 132 ~~and droplets act as sources of LWC (or LWP).~~ More ice crystals and droplets provide the
 133 greater integrated surface area of ice crystals and droplets and induce more deposition and
 134 condensation, respectively, for a given environmental condition (Lee et al., 2009; Khain et
 135 al., 2012; Fan et al., 2018; Chua and Ming, 2020; Lee et al., 2021). The higher
 136 ICNC/CDNC means more ice crystals or sources of deposition per a droplet as a source of
 137 condensation in a given group of ice crystals and droplets. Thus, the higher ICNC/CDNC
 138 enables more deposition per unit condensation to occur, which can raise IWC/LWC or
 139 IWP/LWP.

140 Mixed-phase stratocumulus clouds in different regions are known to have different
 141 IWC/LWC or IWP/LWP and aerosol-cloud interactions (e.g., Choi et al., 2010 and 2014;
 142 Zhang et al., 2019). Lots of factors such as environmental conditions, which can be
 143 represented by variables such as temperature, humidity and wind shear, and macrophysical
 144 factors one of which is the relative locations of ice-crystal and droplet layers, can explain
 145 those differences. Choi et al. (2010 and 2014) and Zhang et al. (2019) have shown that as
 146 temperature lowers, IWC/LWC or IWP/LWP tends to increase and indicated that
 147 temperature is a primary environmental condition to explain the differences in IWC/LWC
 148 among different regions or clouds. However, Choi et al. (2010 and 2014) and Zhang et al.
 149 (2019) have not discussed process-level mechanisms that govern the role of temperature in
 150 those differences.

151 It is important to establish a general principle that explains the differences in
 152 LWC/LWC and aerosol-cloud interactions among regions, since the general principle is
 153 useful in the development of a more general or comprehensive parameterization of

Deleted: This is because deposition and condensation of water vapor occur on the surface of ice crystals and droplets, respectively.

Deleted: Thus

Deleted: and droplets

Deleted: , respectively

Deleted: Then

Deleted: and droplets

Deleted: and

Deleted: , respectively

163 stratocumulus clouds and their interactions with aerosols for climate models. This
164 contributes to the better prediction of future climate, considering that the absence of the
165 comprehensive parameterization has been considered one of the biggest obstacles to the
166 better prediction (Ramaswamy et al., 2001; Foster et al., 2007; Stevens and Feingold, 2009).

167 As a way of contributing to the establishment of the general principle, this study
168 attempts to take ICNC/CDNC as a general factor, which can constitute the general principle,
169 to explain the differences in IWC/LWC (or IWP/LWP) and aerosol-cloud interactions
170 among clouds. This study also attempts to elucidate how ice processes differentiate mixed-
171 phase stratiform clouds from warm clouds in terms of cloud development and its
172 interactions with aerosols, and how this differentiation varies among cases of mixed-phase
173 stratiform clouds with different ICNC/CDNC values. This attempt is valuable, considering
174 that in general, the establishment of the general principle for stratocumulus clouds and their
175 interactions with aerosols has been progressed much less than that for other types of clouds
176 such as convective clouds and their interactions with aerosols. The attempt is valuable, also
177 considering that our level of understanding of how ice processes differentiate mixed-phase
178 stratiform clouds and their interactions with aerosols from much-studied warm clouds and
179 their interactions with aerosols has been low. Here, we want to emphasize that this study
180 does not aim to gain a fully established general principle, but aims to test the factor that
181 can be useful to move ahead on our path to a more complete general principle. Hence, this
182 study should be regarded a steppingstone to the established principle, and should not be
183 considered a perfect study that get us the fully established principle. Taking into account
184 the fact that even attempts to provide general factors for the general principle have been
185 rare, the fulfilment of the aim is likely to provide us with valuable preliminary information
186 that streamlines the development of a more established general principle.

187 For the attempt, this study investigates a case of mixed-phase stratiform clouds in the
188 polar region. Via the investigation, this study aims to identify process-level mechanisms
189 that control the development of those clouds and their interactions with aerosols, and the
190 impact of ice processes on the development and interactions using a large-eddy simulation
191 (LES) framework. Then, this study compares the mechanisms in the case of polar clouds
192 to those in a case of midlatitude clouds which have been examined by Lee et al. (2021).
193 This comparison is based on Choi et al. (2010 and 2014) and Zhang et al. (2019) which

194 have shown that temperature is an important factor which explains the differences in
195 IWC/LWC among regions or clouds. Due to significant differences in latitudes, noticeable
196 differences in the temperature of air are between the polar and midlatitude cases. Hence,
197 through this comparison, this study looks at the role of temperature in those differences in
198 IWC/LWC and associated aerosol-cloud interactions. More importantly than that, as a way
199 of identifying process-level mechanisms that control the role of temperature, this study
200 tests how ICNC/CDNC as the general factor is linked to the role of temperature, using the
201 LES framework. Through this test, this study also identifies process-level mechanisms that
202 control how ICNC/CDNC affects roles of ice processes in the differentiation between
203 mixed-phase stratiform and warm clouds in terms of cloud development and its interactions
204 with aerosols, and causes the variation of the differentiation between the cases of mixed-
205 phase stratiform clouds.

206

207 **2. Case, model and simulations**

208

209 **2.1 LES model**

210

211 LES simulations are performed by using the Advanced Research Weather Research and
212 Forecasting (ARW) model. A bin scheme, which is detailed in Khain et al. (2000) and
213 Khain et al. (2011), is adopted by the ARW for the simulation of microphysics. Size
214 distribution functions for each class of hydrometeors, which are classified into water drops,
215 ice crystals (plate, columnar and branch types), snow aggregates, graupel and hail, are
216 represented with 33 mass doubling bins, i.e., the mass of a particle m_k in the k th bin is
217 determined as $m_k = 2m_{k-1}$. Each of hydrometeors has its own terminal velocity that varies
218 with the hydrometeor mass and the sedimentation of hydrometeors is simulated using their
219 terminal velocity.

220 Size distribution functions for aerosols, which act as cloud condensation nuclei
221 (CCN) and ice-nucleating particles (INP), adopt the same mass doubling bins as for
222 hydrometeors. The evolution of aerosol size distribution and associated aerosol
223 concentrations at each grid point is controlled by aerosol sinks and sources such as aerosol
224 advection, turbulent mixing, activation and aerosol regeneration via the evaporation of

225 droplets and the sublimation of ice crystals. Aerosol regeneration follows the method
226 similar to that as described in Xue et al. (2010). It is assumed that aerosols do not fall down
227 by themselves and move around by airflow that is composed of horizontal flow, updrafts,
228 downdrafts and turbulent motions. When aerosols move with airflow, it is assumed that
229 they move with the same velocity as airflow. Taking activation as an example of the
230 evolution of aerosol size distribution, the bins of the aerosol spectra that correspond to
231 activated particles are emptied. Activated aerosol particles are included in hydrometeors
232 and move to different classes and sizes of hydrometeors through collision-coalescence. In
233 case hydrometeors with aerosol particles precipitate to the surface, those particles are
234 removed from the atmosphere.

235 The large energetic turbulent eddies are directly resolved by the LES framework, and
236 the effects of the smaller subgrid-scale turbulent motions on the resolved flow are
237 parameterized based on a most widely used method that Smagorinsky (1963) and Lilly
238 (1967) proposed. In this method, the mixing time scale is defined to be the norm of the
239 strain rate tensor (Bartosiewicz and Duponcheel, 2018). A cloud-droplet nucleation
240 parameterization based on Köhler theory represents cloud-droplet nucleation. Arbitrary
241 aerosol mixing states and aerosol size distributions can be fed to this parameterization. To
242 represent heterogeneous ice-crystal nucleation, the parameterizations by Lohmann and
243 Diehl (2006) and Möhler et al. (2006) are used. In these parameterizations, contact,
244 immersion, condensation-freezing, and deposition nucleation paths are all considered by
245 taking into account the size distribution of INP, temperature and supersaturation.
246 Homogeneous aerosol (or haze particle) and droplet freezing is
247 also considered following the theory developed by Koop et al. (2000).

248 The bin microphysics scheme is coupled to the Rapid Radiation Transfer Model
249 (RRTM; Mlawer et al., 1997). The effective sizes of hydrometeors, which are calculated
250 in the bin scheme, are fed into the RRTM as a way of considering effects of the effective
251 sizes on radiation. The surface process and resultant surface heat fluxes are simulated by
252 the interactive Noah land surface model (Chen and Dudhia, 2001).

253

254 **2.2 Case and simulations**

255

2.2.1 Case and standard simulations

256

257

258 In the Svalbard area, Norway, a system of mixed-phase stratocumulus clouds existed over
 259 the horizontal domain marked by a red rectangle in Figure 1 and a period between 02:00
 260 and 10:00 local solar time (LST) on March 29th, 2017. These clouds are observed by a
 261 ground station which is a part of the Cloudnet observation network and marked by a dot in
 262 Figure 1. The Cloudnet observation has been established to provide a systematic evaluation
 263 of clouds in forecast and climate models. The Cloudnet observation aims to establish a
 264 number of ground-based remote sensing sites, which would all be equipped with a specific
 265 array of instrumentation, using sensors such as radiometer, lidar and Dopplerized mm-
 266 wave radar, in order to provide vertical profiles of the main cloud variables (e.g., LWC and
 267 IWC) (Hogan et al., 2006). In the Cloudnet observation, particularly, LWC is measured by
 268 radiometer with a spatial resolution of ~50 m in the vertical direction and a temporal
 269 resolution of 30 seconds. The retrieval of IWC is performed by using radar reflectivity and
 270 lidar backscatter in the Cloudnet observation with a spatial resolution of ~10 m in the
 271 vertical direction and a temporal resolution of 30 seconds as described in Donovan et al.
 272 (2001), Donovan and Lammeren (2001), Donovan (2003) and Tinel et al. (2005). In the
 273 retrieval, the lidar signal and radar reflectivity profiles are combined and inverted using a
 274 combined lidar/radar equation as a function of the light extinction coefficient and radar
 275 reflectivity. The combined equation is detailed in Donovan and Lammeren (2001). In the
 276 Cloudnet data, LWC data with the coarser spatial resolution than IWC data are interpolated
 277 to observation locations of IWC data, and IWP and LWP data are obtained from these IWC
 278 and interpolated LWC data, respectively. The Cloudnet observation data including these
 279 IWC, LWC, IWP and LWP data are provided to the public with a temporal resolution of
 280 30 seconds in a continuous manner. This study utilizes these publicized Cloudnet data.

281 On average, the bottom and top of the observed clouds, which are measured by radar
 282 and lidar in the Cloudnet observation, are at ~400 m and ~3 km in altitude, respectively.
 283 The simulation of the observed system or case, i.e., the control run, is performed three-
 284 dimensionally over the red rectangle and the period between 02:00 and 10:00 LST on
 285 March 29th, 2017. The horizontal domain adopts a 100-m resolution for the control run. The
 286 length of the domain in the horizontal directions is 50 km. The length of the domain in the

Deleted: ground

Deleted: that

Deleted: active

Deleted: P

Deleted: P

Deleted:)

Deleted: , at high spatial and temporal resolution

Deleted: The Cloudnet observation provides data of important cloud variables such as LWP and IWP to the public

Moved (insertion) [2]

Deleted: P

Deleted: and

Deleted: t

299 vertical direction is ~ 5 km and the resolution for the vertical domain gets coarsened with
300 height from ~ 5 m just above the surface to ~ 150 m at the model top as detailed in the
301 supplement. Reanalysis data, which are produced by Met Office Unified Model (Brown et
302 al., 2012) every 6 hours on a $0.11^\circ \times 0.11^\circ$ grid, provide potential temperature, specific
303 humidity, and wind as initial and boundary conditions, which represent synoptic-scale
304 environment, for the control run. The control run employs an open lateral boundary
305 condition. Figure 2a shows the vertical distribution of the domain-averaged potential
306 temperature and humidity in those reanalysis data at the first time step. A neutral, mixed
307 layer is between the surface and 1 km in altitude as an initial condition (Figure 2a). Figure
308 2b shows the time evolution of the domain-averaged large-scale subsidence or downdraft
309 in the reanalysis data and at the model top. This large-scale subsidence is imposed on the
310 control run as a part of background wind fields and interacts with updrafts and downdrafts
311 generated by relatively small-scale processes including those associated with clouds. The
312 large-scale subsidence gradually reduces with time (Figure 2b). Figure 2c shows the time
313 evolution of the domain-averaged surface temperature in the reanalysis data. This evolution
314 of the surface temperature is strongly controlled by the sea surface temperature considering
315 that a large portion of the red-rectangle domain is accounted for by the ocean (Figure 1).
316 Due to the sunrise, the surface temperature starts to increase more rapidly around 08:00
317 LST (Figure 2c).

318 The properties of cloud condensation nuclei (CCN) such as the number concentration,
319 size distribution and composition are measured in the domain (Tunved et al., 2013; Jung et
320 al., 2018). The measurement of the CCN concentration has been carried out at the location
321 marked by a dot in Figure 1, using the commercial droplet measurement technologies CCN
322 counter with one column (CCNC-100), managed by the Korea Polar Research Institute,
323 since year 2007. The CCNC-100 measures the CCN concentration at supersaturations of
324 0.2, 0.4, 0.6, 0.8 and 1% (Jung et al., 2018). The aerosol number size distribution is
325 observed using a closed-loop differential mobility particle sizer (DMPS). The DMPS
326 charges aerosol particles and exposing them into an electric field, which causes them to
327 experience a force proportional to their electrical mobility, resulting in their classification
328 according to size (Tunved et al., 2013). Aerosol composition is measured using aerosol

Deleted: at the Zeppelin research station in the domain

330 mass spectrometry (AMS). The AMS measures the composition by vaporizing and ionizing
331 aerosol particles.

332 The measurement indicates that on average, aerosol particles are an internal mixture
333 of 70 % ammonium sulfate and 30 % organic compound. This mixture is assumed to
334 represent aerosol chemical composition over the whole domain and simulation period for
335 this study. The observed and averaged concentration of aerosols acting as CCN is ~ 200
336 cm^{-3} over the simulation period between 02:00 and 10:00 LST on March 29th, 2017. Note
337 that the average of a variable with respect to time in the rest of this paper is performed over
338 this period between 02:00 and 10:00 LST, unless otherwise stated. 200 cm^{-3} as the averaged
339 concentration of aerosols acting as CCN is interpolated into all of grid points immediately
340 above the surface at the first time step.

341 This study does not take into account aerosol effects on radiation before aerosol is
342 activated, since no significant amount of radiation absorbers is found in the mixture. Based
343 on observation, the size distribution of aerosols acting as CCN is assumed to be a tri-modal
344 log-normal distribution (Figure 3). The shape of distribution, which is a tri-modal log-
345 normal distribution, as shown in Figure 3 is applied to the size distribution of aerosols
346 acting as CCN in all parts of the domain during the whole simulation period. The assumed
347 shape in Figure 3 is obtained by performing the average on the observed size distribution
348 parameters (i.e., modal radius and standard deviation of each of nuclei, accumulation and
349 coarse modes, and the partition of aerosol number among those modes) over the simulation
350 period. Note that although these parameters or the shape of aerosol size distribution does
351 not vary, associated aerosol concentrations vary over the simulation domain and period via
352 processes as described in Section 2.1. This study takes an assumption that the interpolated
353 CCN concentrations do not vary with height in a layer between the surface and the
354 planetary boundary layer (PBL) top around 1 km in altitude at the first time step, following
355 the previous studies such as Gras (1991), Jaenicke (1993) and Seinfeld and Pandis (1998).
356 However, above the PBL top, they are assumed to decrease exponentially with height at
357 the first time step, based on those previous studies, although the shape of size distribution
358 and composition do not change with height. It is assumed that the properties of INP and
359 CCN are not different except for concentrations. The concentration of aerosols acting as
360 CCN is assumed to be 100 times higher than that acting as INP over grid points at the first

361 time step based on a general difference in concentrations between CCN and INP
362 (Pruppacher and Klett, 1978). Hence, the concentration of aerosols acting as INP at the
363 first time step is 2 cm^{-3} in the control run. This assumed concentration of aerosols acting
364 as INP is higher than usual (Seinfeld and Pandis, 1998). However, Hartmann et al. (2021)
365 observed the INP concentration that was at the same order of magnitude as assumed here
366 in the Svalbard area when strong dust events occur, meaning that the assumed INP
367 concentration is not that unrealistic.

368 To examine effects of aerosols on mixed-phase clouds, the control run is repeated by
369 increasing the concentration of aerosols by a factor of 10. In the repeated (control) run, the
370 initial concentrations of aerosols acting as CCN and INP at grid points immediately above
371 the surface are 2000 (200) and $20 \text{ (2)} \text{ cm}^{-3}$, respectively. Reflecting these concentrations in
372 the simulation name, the control run is referred to as “the 200_2 run” and the repeated run
373 is referred to as “the 2000_20 run”. To isolate effects of aerosols acting as CCN (INP) on
374 mixed-phase clouds, the control run is repeated again by increasing the concentration of
375 aerosols acting as CCN (INP) only but not INP (CCN) by a factor of 10. In this repeated
376 run with the increase in the concentration of aerosols acting as CCN (INP), the initial
377 concentrations of aerosols acting as CCN and INP at grid points immediately above the
378 surface are 2000 (200) and $2 \text{ (20)} \text{ cm}^{-3}$, respectively. Reflecting this, the repeated run is
379 referred to as “the 2000_2 (200_20) run”.

380

381 **2.2.2 Additional simulations**

382

383 To isolate impacts of ice processes on the adopted case and its interactions with aerosols,
384 the 200_2 and 2000_2 runs are repeated by removing ice processes. These repeated runs
385 are referred to as the 200_0 and 2000_0 runs. In the 200_0 and 2000_0 runs, all
386 hydrometeors (i.e., ice crystals, snow, graupel, and hail), phase transitions (e.g., deposition
387 and sublimation) and aerosols (i.e., INP) which are associated with ice processes are
388 removed. Hence, in these runs, only droplets (i.e., cloud liquid), raindrops, associated phase
389 transitions (e.g., condensation and evaporation) and aerosols acting as CCN are present,
390 regardless of temperature. Stated differently, these no-ice runs simulate the warm-cloud
391 counterpart of the selected mixed-phase cloud system. Via comparisons between a pair of

392 the 200_2 and 2000_2 runs and a pair of the 200_0 and 2000_0 runs, the role of ice
 393 processes in the differentiation between mixed-phase and warm clouds is to be identified.
 394 Along with this identification, the role of the interplay between ice crystals and droplets in
 395 the development of the selected mixed-phase cloud system and its interactions with
 396 aerosols is to be isolated.

397 As detailed in Sections 3.1.4 and 3.2.2 below, the test of ICNC/CDNC as a general
 398 factor requires more simulations to see impacts of ICNCavg/CDCNavg on clouds and their
 399 interactions with aerosols. Here, ICNCavg and CDNCavg represent the average ICNC and
 400 CDNC over grid points and time steps with non-zero ICNC and CDNC, respectively.
 401 ICNCavg/CDNCavg represents overall ICNC/CDNC over the domain and simulation
 402 period. To respond to this requirement, the 200_0.07, 2000_0.07 and 200_0.7 runs are
 403 performed and their details are given in Sections 3.1.4 and 3.2.2. In addition, all the
 404 simulations above are repeated by turning off radiative processes and Section 3.3 provides
 405 the details of these repeated simulations. These repeated runs are the 200_2_norad,
 406 2000_20_norad, 2000_2_norad, 200_20_norad, 200_0_norad, 2000_0_norad,
 407 200_0.07_norad, 2000_0.07_norad and 200_0.7_norad runs. Moreover, based on the
 408 argument in Section 4.2, the 4000_45, 13_0.1, 4000_1.8 and 12_0.0035 runs are performed
 409 and details of these runs are provided in Section 4.2. Some of the simulations are
 410 summarized in Table 1 for better clarification with a brief description of their configuration.

411

412 3. Results

413

414 3.1 The 200_2 run vs. the 200_0 run

415

416 3.1.1 Model validation

417

418 This study adopts the Cloudnet observation, which has been used to assess cloud
 419 simulations as in Illingworth et al. (2007) and Hansen et al. (2018), to evaluate the 200_2
 420 run. Simulated LWP and IWP, as shown in Figure 4 and Table 2, are compared to the
 421 observed LWP and retrieved IWP in the Cloudnet data, respectively. The average LWP
 422 over all time steps and grid columns for the period between 02:00 and 10:00 LST on March

Deleted: ground

Moved up [2]: The retrieval of IWP is performed by using radar reflectivity and lidar backscatter in the Cloudnet observation as described in Donovan et al. (2001), Donovan and Lammeren (2001), Donovan (2003) and Tinel et al. (2005). In the retrieval, the lidar signal and radar reflectivity profiles are combined and inverted using a combined lidar/radar equation as a function of the light extinction coefficient and radar reflectivity. The combined equation is detailed in Donovan and Lammeren (2001).

Deleted: Observed LWP is provided by radiometer in the Cloudnet observation.

434 29th, 2017 is 1.23 g m^{-2} in the 200_2 run and 1.12 g m^{-2} in the Cloudnet observation. The
 435 average IWP over all time steps and grid columns over the period is 31.94 g m^{-2} in the
 436 200_2 run and 29.10 g m^{-2} in the retrieval. Cloud-bottom height, which is averaged over
 437 grid columns and time steps with non-zero cloud-bottom height over the period, is 420 m
 438 in the 200_2 run and 440 m in the Cloudnet observation. Cloud-top height, which is
 439 averaged over grid columns and time steps with non-zero cloud-top height over the period,
 440 is 3.5 km in the 200_2 run and 3.3 km in the Cloudnet observation. Each of LWP, cloud-
 441 bottom and -top heights shows an $\sim 10\%$ difference between the 200_2 run and observation.
 442 IWP also shows an $\sim 10\%$ difference between the 200_2 run and the retrieval. Thus, the
 443 200_2 run is considered performed reasonably well for these variables.

444 To provide additional information of cloud development, Figure 5 shows the time
 445 evolution of the simulated and observed cloud-top and bottom heights, simulated and
 446 retrieved IWP and simulated and observed LWP together with the evolution of the
 447 simulated surface sensible and latent-heat fluxes; the simulated evolutions in Figure 5 are
 448 from the 200_2 run. This is based on the fact that the cloud-top and bottom heights, IWP
 449 and LWP are considered a good indicative of cloud development and the surface fluxes are
 450 considered important parameters controlling the overall development of clouds. The cloud-
 451 top height increases between 02:00 and $\sim 05:00$ LST and after $\sim 05:00$ LST, it reduces
 452 gradually. The cloud-bottom height decreases between 02:00 and $\sim 05:00$ LST and after
 453 $\sim 05:00$ LST, it does not change much. IWP and LWP show an overall increase between
 454 02:00 and $\sim 05:30$ LST to reach its peak around 05:30 LST and then an overall decrease.
 455 The surface fluxes reduce with time, although the reduction rate of the fluxes starts to
 456 decrease around 08:00 LST in association with the rapid increase in the surface temperature
 457 which starts around 08:00 LST as shown in Figure 2c.

458 The time- and domain-averaged IWP is \sim one order of magnitude greater than LWP, and
 459 the time- and domain-averaged IWC is \sim one order of magnitude greater than LWC in the
 460 200_2 run (Figure 4 and Table 2). For the sake of simplicity, the averaged IWC over the
 461 averaged LWC is denoted by IWC/LWC , and the averaged IWP over the averaged LWP
 462 is by IWP/LWP , henceforth. IWC/LWC is 26.28 and IWP/LWP is 25.96 in the 200_2 run.
 463 Since IWP and LWP are vertically integrated IWC and LWC over the vertical domain,
 464 respectively, the qualitative nature of differences between IWC and LWC is not much

Deleted: 200_2 run and

Deleted: , respectively

Deleted:

Deleted: 200_2 run and

Deleted: , respectively

Deleted: and IWC are \sim one order of magnitude greater than LWP and LWC, respectively,

Deleted: and IWP/LWP

Deleted: are

Deleted: , respectively,

475 different from that between IWP and LWP. Hence, mentioning both a pair of IWC and
 476 LWC and that of IWP and LWP is considered redundant, and mentioning either a pair of
 477 IWC and LWC or that of IWP and LWP enhances the readability. Henceforth, IWC and
 478 LWC are chosen to be mentioned in text, although all of IWC, LWC, IWP and LWP are
 479 displayed in Tables 2 and 3.

480 _Choi et al. (2014) and Zhang et al. (2019) have obtained the supercooled cloud fraction
 481 (SCF), which is basically the ratio of LWC to the sum of LWC and IWC and denoted by
 482 $LWC/(LWC+IWC)$, using satellite- and ground-observed data collected over the period of
 483 ~1 year to ~5 years. Choi et al. (2014) have shown that SCF is as low as ~0.01 for the
 484 temperature range between -16 and -33 °C. Zhang et al. (2019) have also shown that SCF
 485 is as low as ~0.03 for the same temperature range, although the occurrence of SCF of ~0.03
 486 or lower is rare. Note that the average air temperature immediately below the cloud base
 487 and above the cloud top over the simulation period is -16 and -33 °C, respectively, in the
 488 200_2 run, and SCF in the 200_2 run is 0.04. Hence, based on Choi et al. (2014) and Zhang
 489 et al. (2019), we believe that SCF in the 200_2 run is observable and thus not that
 490 unrealistic, although it may not occur frequently.

Deleted: and ~1 year, respectively

491

492 3.1.2 Microphysical processes, sedimentation and entrainment

493

494 To understand process-level mechanisms that control the results, microphysical processes
 495 are analyzed. As indicated by Ovchinnikov et al. (2011), in clouds with weak precipitation,
 496 a high-degree correlation is found between IWC and deposition or between LWC and
 497 condensation, considering that deposition is the source of IWC and condensation is the
 498 source of LWC. In the 200_2 run, the average surface precipitation rate over the simulation
 499 period is ~0.0020 mm hr⁻¹, which can be considered weak. Hence, in this case,
 500 condensation is considered a proxy for LWC, and deposition is a proxy for IWC. Based on
 501 this, to gain a process-level understanding of microphysical processes that control the
 502 simulated LWC and IWC, condensation and deposition are analyzed.

Deleted: and condensation are sources of IWC and LWC, respectively. ...

Deleted: and deposition are considered proxies for LWC and IWC, respectively.

503 As seen in Figure 6 and Table 2, the average deposition rate is ~one order of magnitude
 504 greater than condensation rate in the 200_2 run, leading to much greater IWC than LWC
 505 in the 200_2 run. This is in contrast to the situation in the case of mixed-phase

511 stratocumulus clouds, which were located in a midlatitude region, in Lee et al. (2021). In
512 that case, the average IWC and LWC are at the same order of magnitude. For the sake of
513 brevity, the case in Lee et al. (2021) is referred to as “the midlatitude case”, while the case
514 of mixed-phase clouds, which is adopted by this study, in the Svalbard area is referred to
515 “the polar case”, henceforth. In the midlatitude case, IWC/LWC is 1.55, which is ~ one
516 order of magnitude smaller than that in the polar case.

517 Warm clouds in the 200_0 run shows that the time- and domain-averaged condensation
518 rate that is lower than the time- and the domain-averaged sum of condensation and
519 deposition rates in the 200_2 run (Figure 6 and Table 2). This leads to a situation where
520 warm clouds in the 200_0 run shows the time- and domain-averaged LWC that is lower
521 than the time- and domain-averaged water content (WC), which is the sum of IWC and
522 LWC, in mixed-phase clouds in the 200_2 run (Figure 4 and Table 2). This is despite the
523 fact that LWC in the 200_0 run is higher than LWC in the 200_2 run (Figure 4 and Table
524 2); WC represents the total cloud mass in mixed-phase clouds, while LWC alone represents
525 the total cloud mass in warm clouds.

526 It should be noted that the average rate of sedimentation of droplets over the cloud
527 base and simulation period reduces from the 200_0 run to the 200_2 run (Table 2). This is
528 mainly due to the decrease in LWC from the 200_0 run to the 200_2 run. The average rate
529 of sedimentation of ice crystals over the cloud base and simulation period increases from
530 the 200_0 run to the 200_2 run, since sedimentation of ice crystals is absent in the 200_0
531 run (Table 2). The average entrainment rate over the cloud top and simulation period
532 increases from the 200_0 run to the 200_2 run (Table 2). Here, entrainment rate is defined
533 to be the difference between the rate of increase in cloud-top height and the large-scale
534 subsidence, following Moeng et al. (1999), Jiang et al. (2002), Stevens et al. (2003a and
535 2003b) and Ackerman et al. (2004). Entrainment tends to reduce the total cloud mass more
536 in the 200_2 run than in the 200_0 run. Thus, entrainment should be opted out when it
537 comes to mechanisms leading to the increase in the total cloud mass from the 200_0 run to
538 the 200_2 run. Here, the vertical integration of each of condensation and deposition rates
539 is obtained over each cloudy column in the domain for each of the runs. For the sake of the
540 brevity, this vertical integrations of condensation and deposition rates are referred to as the
541 integrated condensation and deposition rates, respectively. Then, each of the integrated

542 condensation and deposition rates is averaged over cloudy columns and the simulation
 543 period. It is found that the average rate of the droplet sedimentation over the cloud base
 544 and simulation period is ~four orders of magnitude smaller than the average integrated
 545 condensation rate in the 200_2 run (Table 2). The average rate of the ice-crystal
 546 sedimentation over the cloud base and simulation period is ~four orders of magnitude
 547 smaller than the average integrated deposition rate in the 200_2 run (Table 2). It is also
 548 found that the average rate of the droplet sedimentation over the cloud base and simulation
 549 period is ~five orders of magnitude smaller than that in the average integrated condensation
 550 rate in the 200_0 run (Table 2). Changes in the average rate of the droplet sedimentation
 551 over the cloud base and simulation period are ~four to five orders of magnitude smaller
 552 than those in the average integrated condensation rate between the 200_2 and 200_0 runs
 553 (Table 2). Changes in the average rate of the ice-crystal sedimentation over the cloud base
 554 and simulation period are ~four to five orders of magnitude smaller than those in the
 555 average integrated deposition rate between the 200_2 and 200_0 runs (Table 2). Thus,
 556 condensation and deposition, but not the droplet and ice-crystal sedimentation, are main
 557 factors controlling cloud mass, which is represented by LWC and IWC, and the total cloud
 558 mass in the 200_2 and 200_0 runs. The variation of cloud mass and the total cloud mass
 559 between the runs are also mainly controlled by condensation and deposition, but not by
 560 droplet and ice-crystal sedimentation. These dominant roles of condensation and
 561 deposition over those of droplet and ice-crystal sedimentation are observed in the
 562 midlatitude case and its warm-cloud counterpart as well.

563 3.1.3 Hypothesis

564 We hypothesized that ICNC/CDNC can be an important factor that determines above-
 565 described differences between the polar and midlatitude cases. Note that both in the polar
 566 and midlatitude cases, pockets of ice particles and those of liquid particles are mixed
 567 together instead of being separated from each other as seen in Figure 4 and Lee et al. (2021).
 568 Remember that ice crystals are more as sources of deposition per a droplet when
 569 ICNC/CDNC is higher. Thus, as ICNC/CDNC increases in a situation where $q_v > q_{sw}$, it
 570 is likely that the portion of water vapor, which is deposited onto ice crystals, increases.

Deleted: s

Deleted: and ice-crystal sedimentation over the cloud base and simulation period are ~four orders of magnitude smaller than the average integrated condensation and deposition rates, respectively, in the 200_2 run (Table 2).

Deleted: s

Deleted: and ice-crystal sedimentation over the cloud base and simulation period are ~four to five orders of magnitude smaller than those in the average integrated condensation and deposition rates between the 200_2 and 200_0 runs (Table 2).

Deleted: ,

Deleted: and

Deleted: t

Deleted: as are in the

Deleted: .

Deleted: when

Deleted: is higher

Deleted: and

Deleted: more

Deleted: more

593 ~~This is by stealing water vapor, which is supposed to be condensed onto droplets, from~~
 594 ~~droplets in an air parcel. Here, q_v and q_{sw} represent water-vapor pressure and water-vapor~~
 595 ~~saturation pressure for liquid water or droplets, respectively. As ICNC/CDNC increases in~~
 596 ~~a situation where, $q_{si} < q_v < q_{sw}$, the number of ice crystals, which absorb water vapor,~~
 597 ~~increases per a droplet; here, water vapor absorbed by ice crystals includes that which is~~
 598 ~~produced by droplet evaporation, and, q_{si} represents water-vapor saturation pressure for ice~~
 599 ~~water or ice crystals. Thus, as ICNC/CDNC increases, it is likely that the portion of water~~
 600 ~~vapor, which is deposited onto ice crystals in an air parcel, increases as shown in Lee et al.~~
 601 ~~(2021). This is aided by the higher capacitance of ice crystals than that of droplets~~
 602 ~~(Pruppacher and Klett, 1978). Figure 7 shows the time series of the averaged~~
 603 ~~supersaturation over grid points where deposition occurs in the presence of both droplets~~
 604 ~~and ice crystals in the 200_2 run. Figure 7 indicates that on average, supersaturation occurs~~
 605 ~~for both droplets and ice crystals over those grid points. Hence, on average, the above-~~
 606 ~~described situation of $q_v > q_{sw}$ is applicable to deposition when droplets and ice crystals~~
 607 ~~coexist in the 200_2 run.~~

608 ICNC_{avg}/CDNC_{avg} is 0.22 in the control run (i.e., the 200_2 run) for the polar case
 609 and 0.019 in the control run for the midlatitude case which is described in Lee et al. (2021).
 610 Henceforth, the control run for the midlatitude case is referred to as the control-midlatitude
 611 run. ICNC_{avg}/CDNC_{avg} is ~one order of magnitude higher for the polar case than for the
 612 midlatitude case. This is despite the fact that the ratio of the initial number concentration
 613 of aerosols acting as INP to that of acting as CCN is identical between the 200_2 and
 614 control-midlatitude runs. In addition, identical model, model setup such as vertical
 615 resolutions, and source of reanalysis data are used between the 200_2 and control-
 616 midlatitude runs. However, there are differences in environmental conditions (e.g.,
 617 temperature), cloud macrophysical variables such as cloud-top height and horizontal
 618 resolutions between the runs. Here, while taking these similarities and differences into
 619 account, we hypothesize that the significant differences in ICNC_{avg}/CDNC_{avg} between
 620 runs are mainly due to the fact that ice nucleation strongly depends on air temperature
 621 (Pruppacher and Klett, 1978). When supercooling is stronger, in general, more ice crystals
 622 are nucleated for a given group of aerosols acting as INP. The average air temperature
 623 immediately below the cloud base over the simulation period is -16 °C in the 200_2 run

Deleted:

Deleted: When

Deleted: s higher

Deleted: and

Deleted: more ice crystals can absorb

Deleted: ,

Deleted: including that which is produced by droplet evaporation,

Deleted: ;

Deleted:

Deleted: with higher

Deleted: more

Deleted: more

Deleted: ,

Deleted: although

638 and -5 °C in the control-midlatitude run. The average air temperature immediately above
639 the cloud top is -33 °C in the 200_2 run and -15 °C in the control-midlatitude run. Hence,
640 supercooling is greater and this contributes to the higher ICNCavg/CDNCavg in the polar
641 case than in the midlatitude case. The higher ICNCavg/CDNCavg is likely to induce more
642 portion of water vapor to be deposited onto ice crystals in the polar case than in the
643 midlatitude case. It is hypothesized that this in turn enables IWC/LWC in the 200_2 run to
644 be one order of magnitude greater than that in the control-midlatitude run or in the
645 midlatitude case. Much higher IWC than LWC, which results in a much higher IWC/LWC
646 in the polar case than in the midlatitude case, in the 200_2 run overcomes lower LWC in
647 the 200_2 run than that in the 200_0 run, which leads to the greater total cloud mass in the
648 200_2 run than in the 200_0 run (Figure 4 and Table 2). However, IWC whose magnitude
649 is similar to the magnitude of LWC, which results in a much lower IWC/LWC in the
650 midlatitude case than in the polar case, in the midlatitude case is not able to overcome
651 lower LWC in the midlatitude case than that in the midlatitude warm clouds, which leads
652 to the greater total cloud mass in the midlatitude warm clouds than in the midlatitude case;
653 here, the midlatitude warm clouds are generated by removing ice processes in the
654 midlatitude case. This means that associated with higher ICNC/CDNC and IWC/LWC, ice
655 processes enhance the total cloud mass for the polar case as compared to that for the polar
656 warm-cloud counterpart. However, in the midlatitude case, associated with lower
657 ICNC/CDNC and IWC/LWC, ice processes reduce the total cloud mass as compared to
658 that for the midlatitude warm-cloud counterpart.

659

660 **3.1.4 Role of ICNC/CDNC**

661

662 To test the hypothesis above about the role of ICNC/CDNC in above-described differences
663 between the polar and midlatitude cases, the 200_2 run is repeated by reducing
664 ICNCavg/CDNCavg by a factor of 10. This is done by reducing the concentration of
665 aerosols acting as INP but not CCN in a way that ICNCavg/CDNCavg is lower by a factor
666 of 10 in the repeated run than in the 200_2 run. In this way, this repeated run has
667 ICNCavg/CDNCavg at the same order of magnitude as that in the control-midlatitude run.
668 This repeated run is referred to as the 200_0.07 run. As shown in Figure 8 and Table 2, the

669 200_0.07 run shows much lower deposition rate and IWC than the 200_2 run does.
670 However, as we move from the 200_2 run to the 200_0.07 run, the time- and domain-
671 averaged condensation rate and LWC increases (Figure 8 and Table 2). This is because
672 reduction in deposition increases the amount of water vapor, which is not consumed by
673 deposition but available for condensation. Associated with this, in the 200_0.07 run, the
674 time- and domain-averaged deposition rate and IWC become similar to the average
675 condensation rate and LWC, respectively (Figure 8 and Table 2). Hence, IWC/LWC
676 reduces from 26.28 in the 200_2 run to 1.05 in the 200_0.07 run as ICNCavg/CDNCavg
677 reduces from the 200_2 run to the 200_0.07 run. Here, IWC/LWC in the 200_0.07 run is
678 similar to that in the midlatitude-control run, which demonstrate that the difference in
679 ICNC/CDNC is able to explain the difference in IWC/LWC between the polar and
680 midlatitude cases. It is notable that the reduction in deposition is dominant over the increase
681 in condensation with the decrease in ICNCavg/CDNCavg. Hence, the sum of condensation
682 and deposition rates and WC reduce from the 200_2 run to the 200_0.07 run. That the sum
683 of condensation and deposition rates and WC reduce in a way that the sum and WC in the
684 mixed-phase clouds in the 200_0.07 run are lower than condensation rate and LWC,
685 respectively, in the warm clouds in the 200_0 run is also notable (Figure 8 and Table 2).
686 This is similar to the situation in the midlatitude case and thus demonstrates that the
687 different relation between the mixed-phase and warm clouds can be associated with the
688 difference in ICNC/CDNC between the polar and midlatitude cases.

689 The rate of the sedimentation of ice crystals at the cloud base reduces as
690 ICNCavg/CDNCavg reduces between the 200_2 and 200_0.07 runs, mainly due to
691 reduction in the ice-crystal mass (Table 2). The rate of droplet sedimentation at the cloud
692 base increases as ICNCavg/CDNCavg reduces mainly due to increases in droplet mass and
693 size in association with the increases in LWC (Table 2). The entrainment rate at the cloud
694 top reduces as ICNCavg/CDNCavg reduces (Table 2). It is found that those changes in the
695 average rates of the droplet and ice-crystal sedimentation over the cloud base and
696 simulation period are ~four to five orders of magnitude smaller than those in the average
697 integrated condensation and deposition rates between the 200_2 and 200_0.07 runs (Table
698 2). The entrainment tends to reduce the total cloud mass or WC less with the reducing
699 ICNCavg/CDNCavg. Hence, changes in the entrainment counters the decrease in WC with

700 the reducing ICNCavg/CDNCavg between the 200_2 and 200_0.07 runs. Here, we see that
701 changes in the entrainment are not factors that lead to the increase in LWC, and the
702 decrease in IWC, and eventually the decrease in WC with the reducing
703 ICNCavg/CDNCavg. The analysis of the sedimentation and entrainment exclude them
704 from factors inducing above-described differences between the 200_2 and 200_0.07 runs.
705 Instead, this analysis grants confidence in the fact that deposition and condensation, which
706 are strongly dependent on ICNC/CDNC, are main factors inducing those differences.

707

708 **3.2 Aerosol-cloud interactions**

709

710 Comparisons between the 200_2 and 2000_20 runs show that with the increasing
711 concentration of both of aerosols acting as CCN and those as INP, IWC increases but LWC
712 decreases in the polar case (Figures 9 and Table 2). These decreases in LWC are negligible
713 as compared to these increases in IWC. Hence, the increases in IWC outweigh the
714 decreases in LWC, leading to aerosol-induced increases in WC (Figures 9 and Table 2).
715 To identify roles of specific types of aerosols in these aerosol-induced changes,
716 comparisons not only between the 200_2 and 200_20 runs but also between the 200_2 and
717 2000_2 runs are performed. Comparisons between the 200_2 and 200_20 runs show that
718 the increasing concentration of aerosols acting as INP induces increases in IWC but
719 decreases in LWC (Figure 9 and Table 2). The magnitudes of these increases and decreases
720 are similar to those between the 200_2 and 2000_20 runs (Figure 9 and Table 2). However,
721 comparisons between the 200_2 and 2000_2 runs show that the increasing concentration
722 of aerosols acting as CCN induces negligible changes in either IWC or LWC. Thus, CCN-
723 induced changes in the total cloud mass are negligible, although the increasing
724 concentration of aerosols acting as CCN induces a slight decrease in IWC, and a slight
725 increase in LWC (Figure 9 and Table 2). This demonstrates that INP plays a much more
726 important role than CCN when it comes to the response of the total cloud mass to increasing
727 aerosol concentrations. However, in the midlatitude case, the increasing concentration of
728 aerosols acting as CCN generates changes in the mass as significantly as the increasing
729 concentration of aerosols acting as INP does.

730 To identify roles played by ice processes in aerosol-cloud interactions, a pair of the
 731 200_0 and 2000_0 runs are analyzed and compared to the previous four standard
 732 simulations (i.e., the 200_2, 200_20, 2000_2 and 2000_20 runs). The CCN-induced
 733 increases in LWC in those noise runs are much greater than the CCN-induced changes in
 734 WC in the 200_2 and 2000_2 runs (Figure 9 and Table 2). However, these CCN-induced
 735 increases in LWC in the noise runs are smaller than the INP-induced increases in WC in
 736 the 200_2 and 200_20 runs (Figure 9 and Table 2). This is different from the midlatitude
 737 case where changes in the total cloud mass, whether they are induced by the increasing
 738 concentration of aerosols acting as CCN or INP, in the mixed-phase clouds are much lower
 739 than those CCN-induced changes in the warm clouds.

740

741 3.2.1 Deposition, condensation, sedimentation and entrainment

742

743 The CCN-induced increases **in condensation rates** and decreases **in deposition rates** are
 744 negligible. This leads to the CCN-induced negligible increases **in LWC** and **negligible**
 745 decreases **in IWC** between the 200_2 and 2000_2 runs (Figure 9 and Table 2). However,
 746 between the 200_2 and 200_20 runs, rather the significant INP-induced increases are in
 747 deposition rate, leading to the significant INP-induced increases in IWC (Figure 9 and
 748 Table 2). Between the 200_2 and 200_20 runs, INP-induced decreases in condensation
 749 rate are negligible, leading to the negligible INP-induced decreases in LWC, as compared
 750 to the INP-induced increases in deposition rate and IWC (Figure 9 and Table 2). With the
 751 increasing concentration of aerosols acting as INP from the 200_2 run to the 200_20 run,
 752 the sedimentation of ice crystals at the cloud base decreases (Table 2). This is mainly due
 753 to decreases in the size of ice crystals in association with increases INP and resultant
 754 increases in ICNC. In Figure 10a, we see that the number concentration of ice crystals with
 755 diameters smaller and larger than ~40 micron increases and decreases, respectively, as we
 756 move from the 200_2 run to the 200_20 run, which indicate a shift of the sizes of ice
 757 crystals to smaller ones. From the 200_2 run to the 200_20 run, the sedimentation of
 758 droplets at the cloud base decreases as shown in Table 2, mainly due to decreases in LWC.
 759 Figure 10b shows that the number concentration of drops decreases throughout almost all
 760 parts of the size range from the 200_2 run to the 200_20 run, which indicates a negligible

Deleted: in condensation

Deleted: and

Deleted: , respectively

Deleted:

Deleted: LWC and

Deleted: , respectively,

767 shift in the drop size but a reduction in LWC. It is found that changes in the average rates
768 of the droplet and ice-crystal sedimentation over the cloud base and simulation period are
769 ~three to four orders of magnitude smaller than those in the average integrated
770 condensation and deposition rates between the 200_2 and 200_20 runs (Table 2). From the
771 200_2 run to the 200_20 run, the entrainment at the cloud top increases (Table 2). Hence,
772 the entrainment reduces WC less in the 200_2 run than in the 200_20 run. Here, we see
773 that changes in entrainment and the sedimentation are not factors that we have to focus on
774 to explain the changes in LWC, IWC and WC between the 200_2 and 200_20 runs.

775 In the warm clouds in the 200_0 and 2000_0 runs, the CCN-induced increases in
776 condensation rate occur, leading to those in LWC (Figure 9 and Table 2). However, the
777 CCN-induced increases in condensation rate in the warm clouds associated with the polar
778 case are lower than the INP-induced increases in deposition rate in the polar case (Table
779 2). This contributes to aerosol-induced smaller changes in the total cloud mass in the polar
780 warm clouds than in the polar mixed-phase clouds. The sedimentation of droplets at the
781 cloud base reduces and the entrainment at the cloud top increases from the 200_0 run to
782 2000_0 run (Table 2). The increasing concentration of aerosols acting as CCN induces
783 increases in CDNC and decreases in the droplet size, leading to the reduction in the droplet
784 sedimentation from the 200_0 run to 2000_0 run. The entrainment counters the CCN-
785 induced increases in LWC from the 200_0 run to 2000_0 run. Hence, the entrainment is
786 not a factor which induces the CCN-induced increases in LWC between the 200_0 and
787 2000_0 runs. As seen in Table 2, the changes in the sedimentation rate is ~three orders of
788 magnitude smaller than those in the integrated condensation rate between the 200_0 and
789 2000_0 runs. Hence, it is not the sedimentation but condensation that we have to look at to
790 explain changes in LWC or WC between the 200_0 and 2000_0 runs.

791

792 **3.2.2 Understanding differences between the polar and midlatitude cases**

793

794 Roughly speaking, the CCN-induced changes in LWC via CCN-induced changes in
795 autoconversion of droplets are proportional to LWC that changing CCN affect, and INP-
796 induced changes in IWC via INP-induced changes in autoconversion of ice crystals are
797 proportional to IWC that changing INPs affect (e.g., Dudhia, 1989; Murakami, 1990; Liu

798 and Daum, 2004; Morrison et al., 2005, 2009 and 2012; Lim and Hong, 2010; Mansell et
799 al. 2010; Kogan, 2013; Lee and Baik, 2017). This is for given environmental conditions
800 (e.g., temperature and humidity) and given CCN- or INP-induced changes in microphysical
801 factors such as sizes and number concentrations of droplets or ice crystals. Hence, in the
802 polar case, with a given much lower LWC than IWC, the changing concentration of
803 aerosols acting as CCN is likely to induce smaller changes in the given LWC via CCN
804 impacts on the droplet autoconversion. This is as compared to changes in the given IWC
805 which are induced by the changing concentration of aerosols acting as INP and thus
806 changing ice-crystal autoconversion.

807 The smaller changes in the given LWC are related to changes in CDNC. These changes
808 in CDNC are initiated by those in droplet autoconversion. The larger changes in the given
809 IWC are related to changes in ICNC. These changes in ICNC are initiated by those in ice-
810 crystal autoconversion. Changes in integrated droplet surface area, which are induced by
811 those in CDNC, initiate those in the given LWC. Changes in integrated ice-crystal surface
812 area, which are induced by those in ICNC, initiate those in the given IWC. Remember that
813 condensation occurs on droplet surface and thus droplets act as a source of condensation,
814 and deposition occurs on ice-crystal surface and thus ice crystals act as a source of
815 deposition. Hence, those changes in CDNC and associated integrated droplet surface area
816 can lead to changes in condensation and thus feedbacks between condensation and updrafts,
817 while those changes in ICNC and associated integrated ice-crystal surface area can lead to
818 changes in deposition and thus feedbacks between deposition and updrafts. The smaller
819 CCN-induced changes in LWC involve changes in CDNC and associated smaller changes
820 in condensation and feedbacks between condensation and updrafts in the polar case. This
821 is as compared to changes in deposition and feedbacks between deposition and updrafts
822 which are associated with the INP-induced changes in ICNC and the related larger INP-
823 induced changes in IWC in the polar case. The smaller CCN-induced changes in LWC
824 involve smaller changes in water vapor that is consumed by droplets in the polar case. The
825 larger INP-induced changes in IWC involve larger changes in water vapor that is consumed
826 by ice crystals in the polar case. This leaves the CCN-induced smaller changes in the
827 amount of water vapor available for deposition, which induce the smaller CCN-induced
828 changes in IWC in the polar case. This is as compared to the INP-induced changes in the

829 amount of water vapor which is available for condensation and associated changes in LWC
830 in the polar case.

831 The lower LWC in the polar warm clouds than IWC in the polar case contributes to the
832 INP-induced greater changes in IWC than the CCN-induced changes in LWC in the polar
833 warm clouds. The lower LWC in the polar case than that in the polar warm clouds
834 contributes to the CCN-induced greater changes in LWC in the polar warm clouds than
835 those in LWC and subsequent changes in IWC in the polar case.

836 In contrast to the situation in the polar case, in the midlatitude case, remember that a
837 given LWC is at the same order of magnitude of IWC. Hence, the CCN- induced changes
838 in LWC and subsequent changes in IWC are similar to the INP-induced changes in IWC
839 and subsequent changes in LWC. The greater LWC in the midlatitude warm cloud than
840 both of LWC and IWC in the midlatitude case contributes to the greater CCN-induced
841 changes in LWC in the midlatitude warm cloud. This is as compared to either the CCN-
842 induced changes in LWC and subsequent changes in IWC or the INP-induced changes in
843 IWC and subsequent changes in LWC in the midlatitude case.

844 To confirm above-described mechanisms in this section, which explain different
845 aerosol-cloud interactions between the polar and midlatitude cases, the 200_0.07 run is
846 repeated by increasing INP by a factor of 10 in the PBL at the first time step. This repeated
847 run is referred to as “the 200_0.7 run. Then, the 200_0.07 run is repeated again by
848 increasing CCN by a factor of 10 in the PBL at the first time step. This repeated run is
849 referred to as the 2000_0.07 run. These repeated runs are to see the response of IWC and
850 LWC to the increasing concentration of aerosols acting as INP and CCN. This is when
851 IWC and LWC are at the same order of magnitude and lower in mixed-phase clouds than
852 LWC in the warm-cloud counterpart as in the 200_0.07 run and midlatitude case.
853 Comparisons between the 200_0.07, 200_0.7 and 2000_0.07 runs show that the INP-
854 induced changes in IWC and LWC are similar to the CCN-induced changes in IWC and
855 LWC, respectively, as in the midlatitude case (Figure 9 and Table 2). These comparisons
856 also show that the CCN-induced changes in LWC in the polar warm cloud are greater
857 (Figure 9 and Table 2). This is as compared to either the CCN-induced changes in LWC
858 and subsequent changes in IWC between the 200_0.07 and 2000_0.07 runs or the INP-
859 induced changes in IWC and subsequent changes in LWC between the 200_0.07 and

860 200_0.7 runs (Figure 9 and Table 2). These comparisons demonstrate that differences in
861 ICNC/CDNC play a critical role in differences in aerosol-cloud interactions between the
862 polar and midlatitude cases, considering that differences in ICNC/CDNC between the
863 200_2 and 200_0.07 runs are at the same order of magnitude of those between the cases.

864

865 **3.3 Radiation**

866

867 Studies (e.g., Ovchinnikov et al., 2011; Possner et al., 2017; Solomon et al., 2018) have
868 focused on radiative cooling and subsequent changes in stability and dynamics as a primary
869 driver for the development of mixed-phase stratocumulus clouds and aerosol-induced
870 changes in LWC and IWC in those clouds. Motivated by these studies, to isolate the role
871 of radiative processes in cloud development and aerosol impacts on LWC and IWC, all of
872 the simulations above are repeated by turning off radiative processes. In these repeated
873 runs, radiative fluxes over the whole domain and simulation period are zero. The basic
874 summary of results from these repeated runs is given in Table 3. As seen in comparisons
875 between Tables 2 and 3, the qualitative nature of results, which are mainly about
876 differences in IWC/LWC, the relative importance of the impacts of INP on IWC and LWC
877 as compared to those impacts of CCN, and how warm and mixed-phase clouds are related
878 between the polar and midlatitude cases, in this study does not vary with whether radiative
879 processes exist or not. This demonstrates that ICNC, CDNC, deposition and condensation
880 but not radiative processes drive results in this study.

881

882 **4. Discussion**

883

884 **4.1 Examination of the role of ICNC/CDNC in IWC/LWC in 200_2, 885 2000_20, 2000_2, 200_20, 200_0.07, 2000_0.07 and 200_0.7 runs**

886

887 So far, comparisons between the set of the 200_2, 2000_20, 2000_2 and 200_20 runs for
888 the polar case and the other set of the 200_0.07, 2000_0.07 and 200_0.7 runs, which
889 represents the midlatitude case, have been mainly utilized to understand the role of
890 ICNC/CDNC. However, even when it comes to all the runs in both the sets, differences in

891 ICNCavg/CDNCavg and IWC/LWC are shown among them (Tables 1 and 2). For more
 892 robust examination of particularly the role of ICNC/CDNC in IWC/LWC, which is
 893 basically about the increase and decrease in ICNC/CDNC inducing the increase and
 894 decrease in IWC/LWC, respectively, as identified from the comparison between the 200_2
 895 and 200_0.07 runs in Section 3.1.4, all the runs in the sets are utilized by ordering them as
 896 shown in Table 4. This ordering is done in a way that as we move from the first run in the
 897 first row to the last run in the last row of Table 4, ICNCavg/CDNCavg increases. Overall,
 898 with increasing ICNCavg/CDNCavg, IWC/LWC increases [in Table 4 as also seen in Figure](#)
 899 [11 that shows IWC/LWC as a function of ICNCavg/CDNCavg based on Table 4. This is](#)
 900 [despite the fact that](#) the increase in IWC/LWC is highly non-linear in terms of the increase
 901 in ICNCavg/CDNCavg as seen in the percentage increases, and a decrease in IWC/LWC
 902 is seen with an increase in ICNCavg/CDNCavg from the 2000_20 run to the 200_2 run
 903 (Table 4 [and Figure 11](#)); this high-degree non-linearity in the increase in IWC/LWC is
 904 associated with the fact that interactions between cloud microphysical, thermodynamic and
 905 dynamic processes are well known to be highly non-linear. Hence, overall, findings
 906 regarding the role of ICNC/CDNC in IWC/LWC from the comparison between the 200_2
 907 and 200_0.07 runs are applicable to all the runs in the sets except for the role between the
 908 2000_20 and 200_2 runs. Here, it is notable that the percentage difference in
 909 ICNCavg/CDNCavg is ~9% between the 2000_20 and 200_2 runs and the smallest among
 910 those differences in Table 4. The other differences are larger than 80%. Hence, the
 911 percentage difference in ICNCavg/CDNCavg for a pair of the 2000_20 and 200_2 runs is
 912 at least ~one order of magnitude smaller than that for the other pairs of the runs in Table 4.
 913 This means that findings from the comparison between the 200_2 and 200_0.07 runs are
 914 not suitable to explain the variation of IWC/LWC among clouds when the variation of
 915 ICNC/CDNC is relatively insignificant. According to Table 4, it seems that the variation
 916 of ICNC/CDNC should be greater than a critical value above which those findings are
 917 useful to account for the IWC/LWC variation among clouds.

918 The high-degree non-linearity in the variation of IWC/LWC is epitomized by the 1706
 919 percent increase in IWC/LWC for the 163 percent increase in ICNCavg/CDNCavg from
 920 the 200_0.7 run to the 2000_2 run. This 1706 percent increase in IWC/LWC is induced by
 921 increases in both the initial number concentrations of CCN and INP between the runs

Deleted: , although

923 (Table 1). In other transition from a simulation in a row to that in the next row in Table 4,
924 there are decreases in both the initial number concentrations of CCN and INP, or there is
925 either a change in the initial number concentration of CCN or INP. When either the initial
926 concentration of CCN or INP changes in the transition, less than a 100% increase in
927 IWC/LWC is shown. The decreases in both the initial number concentrations of CCN and
928 INP, which are from the 2000_20 run to the 200_2 run, result in the decrease in IWC/LWC.
929 Hence, depending on how the initial number concentrations of CCN and INP change, the
930 magnitude and sign of the change in IWC/LWC can vary substantially.

931

932 **4.2 Role of a given ICNC/CDNC in IWC/LWC for different concentrations of** 933 **aerosols acting as INP and CCN**

934

935 Simulations which are compared in Section 4.1 and shown in Table 4 have not only
936 different ICNCavg/CDNCavg but also the different number concentrations of aerosols
937 acting as CCN and INP at the first time step (Table 1). To better isolate particularly the
938 role of ICNC/CDNC in IWC/LWC, we need to show that results in Section 4.1 are valid
939 regardless of the variation of the number concentration of aerosols. For this need, we focus
940 on the 200_2 and 200_0.07 runs, since the primary understanding of the role of
941 ICNC/CDNC in IWC/LWC comes from the comparison between these runs as described
942 in Section 3.1.4. To fulfill the need, each of these runs are repeated by varying the number
943 concentration of aerosols acting as CCN and INP in a way that ICNCavg/CDNCavg does
944 not vary (Tables 1 and 5). The 4000_45 and 13_0.1 runs are the repeated 200_2 run, and
945 the 4000_1.8 and 12_0.0035 runs are the repeated 200_0.07 run (Tables 1 and 5). The set
946 of the 200_2, 4000_45 and 13_0.1 runs is referred to as the polar set, and that of the
947 200_0.07, 4000_1.8 and 12_0.0035 runs is referred to as the midlatitude set in this section.
948 Among the three runs in each of the sets, less than 4% variation of IWC/LWC is shown
949 (Table 5). This less-than-4% variation is so small that the start contrast in IWC/LWC
950 between the 200_2 and 200_0.07 runs as discussed in Section 3.1.4 is also shown between
951 the polar and midlatitude sets (Table 5). Hence, the role of the difference in a given
952 ICNC/CDNC in the difference in IWC/LWC between the 200_2 and 200_0.07 runs as
953 described in Section 3.1.4 is considered robust to the varying concentration of aerosols. ▼

Deleted: ¶

4.3 Role of environmental factors, sedimentation, aerosol sources and advection

This study picks ICNC/CDNC as an important factor which differentiates IWC/LWC and interactions among clouds, aerosols and ice processes in the polar case from those in the midlatitude case. However, this does not mean that no other potential factors, which can explain the variation of IWC/LWC and interactions among clouds, aerosols and ice processes between different clouds, exist. For example, differences in environmental factors (e.g., stability and wind shear) between those different clouds can have an impact on the variation. Particularly, differences in stability and wind shear can initiate those in the dynamic development of turbulence. Then, this subsequently induces differences in the microphysical and thermodynamic development of clouds, IWC/LWC and interactions among clouds, aerosols and ice processes. Hence, factors such as stability and wind shear can have different orders of procedures, which involve dynamics, thermodynamics and microphysics, than ICNC/CDNC in terms of differentiation between different clouds. Thus, different mechanisms controlling the differentiation can be expected regarding factors such as stability and wind shear as compared to ICNC/CDNC. The examination of these different mechanisms among stability, wind shear and ICNC/CDNC deserves future study for more comprehensive understanding of the differentiation or for an above-mentioned more fully established general principle explaining the differentiation.

Another point to make is that the cases in this study have weak precipitation and the associated weak sedimentation of ice crystals and droplets. In mixed-phase clouds with strong precipitation and the sedimentation, they can play roles as important as in-cloud latent-heat processes in IWC/LWC and interactions among clouds, aerosols and ice processes. In those clouds with strong precipitation, the sedimentation can take part in the interplay between ICNC/CDNC and latent-heat processes by affecting cloud mass and associated ICNC and CDNC significantly, and play a role in the differentiation of IWC/LWC and interactions among clouds, aerosols and ice processes when it comes to different cases of mixed-phase clouds. For more generalization of results here as a way to the more fully established general principle, this potential role of sedimentation needs to

Formatted: Font: Bold

Deleted:

Deleted: , which is affected by air temperature and its impacts on ice-crystal nucleation,

Deleted: The polar case is located in the Svalbard area, which is in the Arctic, hence, more specifically, the polar case can be referred to as the Arctic case. Differences in ICNC/CDNC initiate differences in the microphysical properties (e.g., the integrated surface area), and then, subsequently induce those in thermodynamic latent-heat processes (e.g., condensation and deposition), dynamics of clouds, IWC/LWC and interactions among clouds, aerosols and ice processes.

997 be investigated by performing more case studies involving cases with strong precipitation
998 in the future.

999 It should be emphasized that although this study mentions air temperature as a factor
1000 that affects ICNC/CDNC, ICNC/CDNC can be affected by other factors such as sources of
1001 aerosols acting as INP and those acting as CCN, and/or the advection of those aerosols.
1002 Hence, even for cloud systems that develop with a similar air-temperature condition, for
1003 example, when those systems are affected by different sources of aerosols and/or their
1004 different advection, they are likely to have different ICNC/CDNC, IWC/LWC, relative
1005 importance of impacts of INP on IWC and LWC as compared to those impacts of CCN,
1006 and relation between warm and mixed-phase clouds. Regarding factors, which affect
1007 ICNC/CDNC, such as sources and advection of aerosols together with temperature, it
1008 should be noted that while this study utilizes differences in temperature among those
1009 factors to identify cases exhibiting significant disparities in ICNC/CDNC, its primary
1010 objective does not lie in the role of temperature differences in disparities in ICNC/CDNC,
1011 but in comprehending the inherent role of ICNC/CDNC variations themselves in the
1012 discrepancies observed, for example, in IWC/LWC, across diverse cloud systems.

1013

1014 4.4 Mixing of droplets and ice crystals

1015

1016 The representation of mixed-phase clouds in our study relies on the assumption of
1017 homogeneously mixed ice and liquid hydrometeors within the model grid cells, a common
1018 approach in many models. However, recent observational studies (e.g., D'Alessandro et al.,
1019 2021; Korolev and Milbrandt, 2022; Schima et al., 2022; Coopman and Tan, 2023) have
1020 shown that in reality, mixed-phase clouds often exhibit inhomogeneous distributions of ice
1021 and liquid, with distinct pockets or regions of each phase. These observations suggest that
1022 the microphysical processes, such as the Wegener-Bergeron-Findeisen process, may be
1023 influenced by this inhomogeneity, potentially leading to differences in cloud dynamics and
1024 feedbacks compared to what is simulated by models assuming the homogeneous mixing.

1025 While our study, along with the work of Lee et al. (2021), uses a model-based
1026 approach that assumes the homogeneous mixing, it is important to acknowledge that this
1027 representation may not fully capture the complexity observed in real clouds. The

Formatted: Font: Bold

1028 implications of this assumption could affect the accuracy of our simulations, particularly
 1029 in scenarios where phase-transition processes in mixed-phase clouds play a significant role.
 1030 As such, the results presented should be interpreted with this limitation in mind, and further
 1031 work incorporating more detailed representations of inhomogeneous hydrometeor
 1032 distributions may be needed to refine our understanding of mixed-phase cloud processes.

1034 5. Summary and conclusions

1036 In this study, a case of mixed-phase stratiform clouds in a polar area, which is referred to
 1037 as “the polar case” is compared to that in a midlatitude area, which is referred to as “the
 1038 midlatitude case”. This is to gain an understanding of how different ICNC/CDNC plays a
 1039 role in making differences in cloud properties, aerosol-cloud interactions and impacts of
 1040 ice processes on them between two representative areas (i.e., polar and midlatitude areas)
 1041 where mixed-phase stratiform clouds form and develop. Among those cloud properties,
 1042 this study focuses on IWC/LWC that plays an important role in cloud radiative properties.
 1043 To gain the understanding efficiently, the polar case is chosen in a way to make stark
 1044 contrast with the midlatitude case in terms of ICNC/CDNC and IWC/LWC. Although such
 1045 polar cases may be uncommon, the stark contrast provides an opportunity to elucidate
 1046 mechanisms that control the above-mentioned role of different ICNC/CDNC.

1047 Due to lower air temperature, more ice crystals are nucleated, leading to higher
 1048 ICNC/CDNC in the polar case than in the midlatitude case. This higher ICNC/CDNC
 1049 enables the more efficient deposition of water vapor onto ice crystals in the polar case. This
 1050 leads to much higher IWC/LWC in the polar case. The more efficient deposition of water
 1051 vapor onto ice crystals enables the polar mixed-phase clouds to have the greater total cloud
 1052 mass than the polar warm clouds. However, the less efficient deposition of water vapor
 1053 onto ice crystals causes the midlatitude mixed-phase clouds to have less total cloud mass
 1054 than the midlatitude warm clouds. With the increasing ICNC/CDNC from the midlatitude
 1055 case to the polar case, impacts of CCN and INP on the total cloud mass become less and
 1056 more important, respectively.

1057 Previous studies on mixed-phase stratocumulus clouds (e.g., Ovchinnikov et al., 2011;
 1058 Possner et al., 2017; Solomon et al., 2018) have primarily focused on investigating the

Deleted: ¶

Moved up [1]: This study picks ICNC/CDNC, which is affected by air temperature and its impacts on ice-crystal nucleation, as an important factor which differentiates IWC/LWC and interactions among clouds, aerosols and ice processes in the polar case from those in the midlatitude case. The polar case is located in the Svalbard area, which is in the Arctic, hence, more specifically, the polar case can be referred to as the Arctic case. Differences in ICNC/CDNC initiate differences in the microphysical properties (e.g., the integrated surface area), and then, subsequently induce those in thermodynamic latent-heat processes (e.g., condensation and deposition), dynamics of clouds, IWC/LWC and interactions among clouds, aerosols and ice processes. However, this does not mean that no other potential factors, which can explain the variation of IWC/LWC and interactions among clouds, aerosols and ice processes between different clouds, exist. For example, differences in environmental factors (e.g., stability and wind shear) between those different clouds can have an impact on the variation. Particularly, differences in stability and wind shear can initiate those in the dynamic development of turbulence. Then, this subsequently induces differences in the microphysical and thermodynamic development of clouds, IWC/LWC and interactions among clouds, aerosols and ice processes. Hence, factors such as stability and wind shear can have different orders of procedures, which involve dynamics, thermodynamics and microphysics, than ICNC/CDNC in terms of differentiation between different clouds. Thus, different mechanisms controlling the differentiation can be expected regarding factors such as stability and wind shear as compared to ICNC/CDNC. The examination of these different mechanisms among stability, wind shear and ICNC/CDNC deserves future study for more comprehensive understanding of the differentiation or for an above-mentioned more fully established general principle explaining the differentiation. Another point to make is that the cases in this study have weak precipitation and the associated weak sedimentation of ice crystals and droplets. In mixed-phase clouds with strong precipitation and the sedimentation, they can play roles as important as in-cloud latent-heat processes in IWC/LWC and interactions among clouds, aerosols and ice processes. In those clouds with strong precipitation, the sedimentation can take part in the interplay between ICNC/CDNC and latent-heat processes by affecting cloud mass and associated ICNC and CDNC significantly, and play a role in the differentiation of IWC/LWC and interactions among clouds, aerosols and ice processes when it comes to different cases of mixed-phase clouds. For more generalization of results here as a way to the more fully established general principle, this potential role of sedimentation needs to be investigated by performing more case studies involving cases with strong precipitation in the future. ¶

It should be emphasized that although this study mentions air temperature as a factor that affects ICNC/CDNC, ICNC/CDNC can be affected by other factors such as sources of aerosols acting as INP and those acting as CCN, and/or the advection of those aerosols. Hence, even for cloud systems that develop with a similar air-temperature condition, for example, when those systems are affected by different sources of aerosols and/or their different advection, they are likely to have different ICNC/CDNC, IWC/LWC, relative importance of impacts of INP on IWC and LWC as compared to those impacts of CCN, and relation between warm and mixed-phase clouds. Regarding factors, which affect ICNC/CDNC, such as sources and advection of aerosols together with temperature, it should be noted that while this study utilizes differences in temperature among those factors to identify cases exhibiting significant disparities in ICNC/CDNC, its primary objective does not lie in the role of temperature differences in disparities in ICNC/CDNC, but in comprehending the inherent role of ICNC/CDNC variations themselves in the discrepancies observed, for example, in IWC/LWC, across diverse cloud systems. ¶

1126 impacts of cloud-top radiative cooling, entrainment, and sedimentation of ice particles on
1127 these clouds, as well as their interactions with aerosols. However, there are a scarcity of
1128 studies that specifically examine the role of microphysical interactions, involving
1129 processes such as condensation and deposition, as well as factors like cloud-particle
1130 concentrations, between ice and liquid particles in mixed-phase stratocumulus clouds, and
1131 their interactions with aerosols as performed in this study. Therefore, our study contributes
1132 to a more comprehensive understanding of mixed-phase clouds and their intricate interplay
1133 with aerosols.

1134 This study suggests that a microphysical factor, which is ICNC/CDNC, can be a
1135 simplified and useful tool to understand differences among different systems of
1136 stratocumulus clouds in various regions in terms of IWC/LWC and the relative importance
1137 of INP and CCN in aerosol-cloud interactions, and thus to contribute to the development
1138 of general parameterizations of those clouds in various regions for climate models. This
1139 factor can also be a useful tool for a simplified understanding of different roles of ice
1140 processes when mixed-phase clouds are compared to their warm-cloud counterparts in
1141 terms of the cloud development and its interactions with aerosols among those different
1142 systems. It should be noted that warm clouds have been studied much more than mixed-
1143 phase clouds, although mixed-phase clouds play as important roles as warm clouds in the
1144 evolution of climate and its change. This study provides preliminary mechanisms which
1145 differentiate mixed-phase clouds and their interactions with aerosols from their warm-
1146 cloud counterparts, and control the variation of the differentiation in different regions as a
1147 way of improving our understanding of mixed-phase clouds. It should be mentioned that
1148 the efficient way of developing general parameterizations, which are for climate models
1149 and consider all of warm, mixed-phase clouds in various regions and their interactions with
1150 aerosols, can be achieved by just adding those mechanisms to pre-existing
1151 parameterizations of much-studied warm clouds instead of developing brand new
1152 parameterizations from the scratch.

1153 This study finds that the relation between ICNC/CDNC and IWC/LWC is highly non-
1154 linear. This high non-linearity is closely linked to how the number concentrations of CCN
1155 and INP, and associated ICNC/CDNC change. For a specific situation where the
1156 ICNC/CDNC variation is relatively small and both the number concentrations of CCN and

1157 INP reduce, the increase in ICNC/CDNC can reduce IWC/LWC, although it is found that
1158 as a whole, the increase in ICNC/CDNC enhances IWC/LWC. Hence, mechanisms
1159 identified in this study, especially regarding the use of ICNC/CDNC as a simplified and
1160 useful tool to explain differences in IWC/LWC among different cloud systems, are not
1161 complete and entirely general. In addition, results in this study are from only two cases in
1162 two specific locations in the midlatitude and Arctic regions and the more generalization of
1163 these results in this study merits more case studies over more locations in those regions,
1164 for example, in terms of above-mentioned sedimentation intensity, different factors (e.g.,
1165 environmental factors) other than ICNC/CDNC, different sources and advection of
1166 aerosols, the magnitude of the variation of ICNC/CDNC and the way number
1167 concentrations of CCN and INP vary. Hence, findings particularly about relations between
1168 ICNC/CDNC and IWC/LWC in this study should be considered preliminary ones that
1169 initiate future work to streamline the development of the general parameterizations.

1170

1171

1172

1173

1174

1175

1176

1177

1178

1179

1180

1181

1182

1183

1184

1185

1186

1187

1188 **Code/Data source and availability**

1189

1190 Our private computer system stores **private data such as the model code and output, and**
 1191 **the CCN data.** Upon approval from funding sources, the data will be opened to the public.

1192 Projects related to this paper have not been finished, thus, the sources prevent the data from
 1193 being open to the public currently. However, if information on the data is needed, contact
 1194 the corresponding author Seoung Soo Lee (slee1247@umd.edu).

1195 **The Cloudnet and reanalysis data used in this study are publicly available. The**
 1196 **Cloudnet data are obtainable at “<https://cloudnet.fmi.fi/search/data>”, while the reanalysis**
 1197 **data can be obtained by contacting Met Office via “[https://www.metoffice.gov.uk/about-](https://www.metoffice.gov.uk/about-us/contact)**
 1198 **us/contact”**

1199 **Author contributions**

1201 Essential initiative ideas are provided by SSL, CHJ and YJY to start this work. Simulation
 1202 and observation data are analyzed by SSL, CHJ and JU. YZ, JP, MGM and SKS review
 1203 the results and contribute to their improvement. JC provides supports to set up and run
 1204 additional simulations during the review.

1205

1206 **Competing interests**

1207 The authors declare that they have no conflict of interest.

1208

1209 **Acknowledgements**

1210 This study is supported by the National Research Foundation of Korea (NRF) grant funded
 1211 by the Korea government (MSIT) (Nos. NRF2020R1A2C1003215,
 1212 NRF2020R1A2C2011081, NRF2023R1A2C1002367,
 1213 NRF2021M1A5A1065672/KOPRI-PN23011 and 2020R1A2C1013278), and Basic
 1214 Science Research Program through the NRF funded by the Ministry of Education (No.
 1215 2020R1A6A1A03044834).

1216

1217

1218

Deleted: ¶

Deleted: the code/data which are private and used in this study.

Field Code Changed

Deleted: ¶

1227 **References**

- 1228
1229 Ackerman, A., Kirkpatrick, M., Stevens, D., et al.: The impact of humidity above
1230 stratiform clouds on indirect aerosol climate forcing, *Science*, 432, 1014–1017,
1231 <https://doi.org/10.1038/nature03174>, 2004.
- 1232 Albrecht, B. A.: Aerosols, cloud microphysics, and fractional cloudiness, *Science*, 245,
1233 1227–1230, 1989.
- 1234 Bartosiewicz, Y., and Duponcheel, M.: Large eddy simulation: Application to liquid metal
1235 fluid flow and heat transfer . In: Roelofs, Ferry, *Thermal Hydraulics Aspects of Liquid*
1236 *Metal Cooled Nuclear Reactors*, Woodhead Publishing, 2018.
- 1237 Brown, A., Milton, S., Cullen, M., Golding, B., Mitchell, J., and Shelly, A.: Unified
1238 modeling and prediction of weather and climate: A 25-year journey, *B. Am. Meteorol.*
1239 *Soc.*, 93, 1865–1877, 2012.
- 1240 Chen, F., and Dudhia, J.: Coupling an advanced land-surface hydrology model with the
1241 Penn State-NCAR MM5 modeling system. Part I: Model description and
1242 implementation, *Mon. Wea. Rev.*, 129, 569–585, 2001.
- 1243 Choi, Y.-S., Ho, C.-H., Park, C.-E., Storelvmo, T., and Tan, I.: Influence of cloud phase
1244 composition on climate feedbacks, *J. Geophys. Res.*, 119, 3687–3700,
1245 doi:10.1002/2013JD020582, 2014.
- 1246 Choi, Y.-S., Lindzen, R. S., Ho, C.-H., and Kim, J.: Space observations of cold-cloud phase
1247 change, *Proc. Natl. Acad. Sci. U.S.A.*, 107, 11211–11216, 2010
- 1248 Chua, X. R., and Ming, Y.: Convective invigoration traced to warm-rain microphysics,
1249 *Geophys. Res. Lett*, 47, <https://doi.org/10.1029/2020GL089134>, 2020.
- 1250 [Coopman, Q., and Tan, I.: Characterization of the spatial distribution of the thermodynamic](#)
1251 [phase within mixed-phase clouds using satellite observations, *Geophys. Res. Lett.*, 50,](#)
1252 [e2023GL104977, 2023.](#)
- 1253 [D'Alessandro, J. J., McFarquhar, G. M., Wu, W., Stith, J. L., Jensen, J. B., and Rauber, R.](#)
1254 [M.: Characterizing the occurrence and spatial heterogeneity of liquid, ice, and mixed](#)
1255 [phase low-level clouds over the Southern Ocean using in situ observations acquired](#)
1256 [during SOCRATES, *J. Geophys. Res.*, 126, e2020JD034482, 2021.](#)
- 1257 Dione, C., Lohou, F., Lothon, M., Adler, B., Babić, K., Kalthoff, N., Pedruzo-Bagazgoitia,

Deleted: ¶



Formatted: Font: (Asian) Malgun Gothic, Font color: Black

Formatted: Font: (Asian) Malgun Gothic, Font color: Black

Formatted: Font: (Asian) Malgun Gothic, Font color: Black

Formatted: Font: (Default) Times New Roman, (Asian) Malgun Gothic, Font color: Black

Formatted: Font: (Asian) Malgun Gothic, Font color: Black

Formatted: Font: (Asian) Malgun Gothic, Font color: Black

Formatted: Font: (Asian) Malgun Gothic, Font color: Black

Formatted: Font: (Asian) Malgun Gothic, Font color: Black

Formatted: Font: (Asian) Malgun Gothic, Font color: Black

Formatted: Font: (Asian) Malgun Gothic, Font color: Black

- 1264 X., Bezombes, Y., and Gabella, O.: Low-level stratiform clouds and dynamical
1265 features observed within the southern West African monsoon, *Atmos. Chem. Phys.*,
1266 19, 8979–8997, <https://doi.org/10.5194/acp-19-8979-2019>, 2019.
- 1267 Donovan, D. P.: Ice-cloud effective particle size parameterization based on combined lidar,
1268 radar reflectivity, and mean Doppler velocity measurements, *J. Geophys. Res.*, 108,
1269 4573, doi:10.1029/2003JD003469, 2003.
- 1270 Donovan, D. P., and van Lammeren, A. C. A. P.: Cloud effective particle size and water
1271 content profile retrievals using combined lidar and radar observations: 1. Theory and
1272 examples, *J. Geophys. Res.*, 106, 27,425–27,448, 2001.
- 1273 Donovan, D. P., van Lammeren, A.C.A.P., Hogan, R. J., Russchenberg, H. W. J., Apituley,
1274 A., Francis, P., Testud, J., Pelon, J., Quante, M., and Goddard, J. W. F.: Cloud effective
1275 particle size and water content profile retrievals using combined lidar and radar
1276 observations – 2. Comparison with IR radiometer and in situ measurements of ice
1277 clouds, *J. Geophys. Res.*, 106, 27449–27464, 2001.
- 1278 Dudhia, J.: Numerical study of convection observed during the winter monsoon
1279 Experiment using a mesoscale two-dimensional Model, *J. Atmos. Sci.*, 46, 3077–3107,
1280 <https://doi.org/10.1175/1520-0469>, 1989.
- 1281 Fan, J., Rosenfeld, D., Zhang, Y., Giangrande, S. E., Li, Z., Machado, L. A. T., Martin, S.
1282 T., Yang, Y., Wang, J., and Artaxo, P.: Substantial convection and precipitation
1283 enhancements by ultrafine aerosol particles. *Science*, 359, 411–418, 2018
- 1284 Forster, P., et al., Changes in atmospheric constituents and in radiative forcing, in: *Climate*
1285 *change 2007: the physical science basis*, Contribution of working group I to the Fourth
1286 Assessment Report of the Intergovernmental Panel on Climate Change, edited by
1287 Solomon, S., et al., Cambridge Univ. Press, New York, 2007.
- 1288 Gettelman, A., Liu, X., Barahona, D., et al.: Climate impacts of ice nucleation, *J. Geophys.*
1289 *Res.*, 117, D20201, doi:10.1029/2012JD017950, 2012.
- 1290 Gras, J. L.: Southern hemisphere tropospheric aerosol microphysics, *J. Geophys. Res.*, 96,
1291 5345–5356.
- 1292 Hahn, C. J., and Warren, S. G.: A gridded climatology of clouds over land (1971–96) and
1293 ocean (1954–97) from surface observations worldwide, Numeric Data Package NDP-
1294 026EORNL/CDIAC-153, CDIAC, Department of Energy, Oak Ridge, TN, 2007.

- 1295 Hannak, L., Knippertz, P., Fink, A. H., Kniffka, A., and Pante, G.: Why do global climate
 1296 models struggle to represent low-level clouds in the West African summer monsoon?,
 1297 J. Climate, 30, 1665–1687, <https://doi.org/10.1175/JCLI-D-16-0451.1>, 2017
- 1298 Hansen, A., Ament, F., Grutzun, V., and Lammert, A.: Model evaluation by a cloud
 1299 classification based on multi-sensor observations, Geosci. Model Dev. Discuss.,
 1300 <https://doi.org/10.5194/gmd-2018-259>, 2018.
- 1301 Hartmann, D. L., Ockert-Bell, M. E., and Michelsen, M. L.: The effect of cloud type on
 1302 earth's energy balance—Global analysis, J. Climate, 5, 1281–1304, 1992.
- 1303 Hartmann, M., Gong, X., Kecorius, S., van Pinxteren, M., Vogl, T., Welti, A., Wex, H.,
 1304 Zeppenfeld, S., Herrmann, H., Wiedensohler, A., and Stratmann, F.: Terrestrial or
 1305 marine – indications towards the origin of ice-nucleating particles during melt season
 1306 in the European Arctic up to 83.7° N, Atmos. Chem. Phys., 21, 11613–11636,
 1307 <https://doi.org/10.5194/acp-21-11613-2021>, 2021.
- 1308 Hogan, R. J., Illingworth, A. J., O'Connor, E. J., et al.: Cloudnet: Evaluation of model
 1309 clouds using ground-based observations, ECMWF Workshop on parametrization of
 1310 clouds on large-scale models., 2006.
- 1311 Illingworth, A. J., Hogan, R. J., O'Connor, E. J., et al.: Cloudnet - continuous evaluation of
 1312 cloud profiles in seven operational models using ground-based observations, Bull. Am.
 1313 Meteorol. Soc., 88, 883-898, 2007.
- 1314 IPCC: Climate Change: The Physical Science Basis. Contribution of Working Group I to
 1315 the Sixth Assessment Report of the Intergovernmental Panel on Climate Change
 1316 [Masson-Delmotte, V., Zhai, P., Pirani, A., Connors, S. L., Péan, C., Berger, S., Caud,
 1317 N., Chen, Y., Goldfarb, L., Gomis, M. I., Huang, M., Leitzell, K., Lonnoy, E.,
 1318 Matthews, J. B. R., Maycock, T. K., Waterfield, T., Yelekçi, O., Yu, R., and Zhou, B.
 1319 (eds.)]. Cambridge University Press, Cambridge, United Kingdom and New York, NY,
 1320 USA, In press, doi:10.1017/9781009157896, 2021.
- 1321 Jaenicke, R.: Tropospheric aerosols in Aerosol-Cloud-Climate Interactions, Hobbs, P. V.,
 1322 ed., Academic Press, San Diego, CA, pp. 1-31.
- 1323 Jiang, H., Feingold, G. and Cotton, W. R: Simulations of aerosol-cloud-dynamical
 1324 feedbacks resulting from entrainment of aerosol into the marine boundary layer during
 1325 the Atlantic Stratocumulus Transition Experiment, J. Geophys. Res., 107(D24), 4813,

Formatted: Font: Italic

Formatted: Font: Not Bold

- 1326 doi:10.1029/2001JD001502, 2002.
- 1327 Jung, C. H., Yoon, Y. J., Kang, H. J., Gim, Y., Lee, B. Y., Ström, J., Krejci, R., and Tunved,
1328 P.: The seasonal characteristics of cloud condensation nuclei (CCN) in the arctic lower
1329 troposphere, *Tellus B: Chemical and Physical Meteorology*, 70:1, 1513291, [https://doi:
1330 10.1080/16000889.2018.1513291](https://doi:10.1080/16000889.2018.1513291), 2018.
- 1331 Khain, A. P., Ovchinnikov, M., Pinsky, M., Pokrovsky, A. and Krugliak, H.: Notes on the
1332 state-of-the-art numerical modeling of cloud microphysics, *Atmos. Res.*, 55, 159–224,
1333 2000.
- 1334 Khain, A., Pokrovsky, A., Rosenfeld, D., Blahak, U., and Ryzhkoy, A.: The role of CCN in
1335 precipitation and hail in a mid-latitude storm as seen in simulations using a spectral
1336 (bin) microphysics model in a 2D dynamic frame, *Atmos. Res.*, 99, 129–146, 2011.
- 1337 Khain, A. P., Phillips, V., Benmoshe, N., Pokrovsky, A.: The role of small soluble aerosols
1338 in the microphysics of deep maritime clouds, *J. Atmos. Sci.*, 69, 2787–2807, 2012.
- 1339 Knippertz, P., Fink, A. H., Schuster, R., Trentmann, J., Schrage, J. M., and Yorke, C.: Ultra-
1340 low clouds over the southern West African monsoon region, *Geophys. Res. Lett.*, 38,
1341 L21808, <https://doi.org/10.1029/2011GL049278>, 2011.
- 1342 [Korolev, A., and Milbrandt, J.: How are mixed-phase clouds mixed?, *Geophys. Res. Lett.*,
1343 49, e2022GL099578, 2022.](#)
- 1344 Kogan, Y., 2013: A cumulus cloud microphysics parameterization for cloud-resolving
1345 models, *J. Atmos. Sci.*, 70, 1423–1436, <https://doi:10.1175/JAS-D-12-0183.1>, 2013.
- 1346 Koop, T., Luo, B. P., Tsias, A., and Peter, T.: Water activity as the determinant for
1347 homogeneous ice nucleation in aqueous solutions, *Nature*, 406, 611–614.
- 1348 Lee, H., and Baik, J.-J.: A physically based autoconversion parameterization, *J. Atmos. Sci.*,
1349 74, 1599–1616, <https://doi.org/10.1175/JAS-D-16-0207.1>, 2017.
- 1350 Lee S. S., Penner, J. E., and Saleeby, S. M.: Aerosol effects on liquid-water path of thin
1351 stratocumulus clouds, *J. Geophys. Res.*, 114, D07204, doi:10.1029/2008JD010513,
1352 2009.
- 1353 Lee, S. S., et al., Mid-latitude mixed-phase stratocumulus clouds and their interactions with
1354 aerosols: how ice processes affect microphysical, dynamic and thermodynamic
1355 development in those clouds and interactions?, *Atmos. Chem. Phys.*,
1356 <https://doi.org/10.5194/acp-21-16843-2021>, 2021.

Formatted: Font: (Asian) Malgun Gothic, Font color: Black

Formatted: Font: (Asian) Malgun Gothic, Font color: Black

Formatted: Font: (Asian) Malgun Gothic, Font color: Black

Formatted: Font: (Default) Times New Roman, (Asian) Malgun Gothic, Font color: Black

Formatted: Font: (Asian) Malgun Gothic, Font color: Black

Formatted: Font: (Asian) Malgun Gothic, Font color: Black

Formatted: Font: (Asian) Malgun Gothic, Font color: Black

Formatted: Font: (Asian) Malgun Gothic, Font color: Black

Formatted: Font: (Asian) Malgun Gothic, Font color: Black

Formatted: Font: (Asian) Times New Roman, Italic, Font color: Auto

- 1357 Li, J., Carlson, B. E., Yung, Y. L., Lv, D., Hansen, J., Penner, J. E., Liao, H., Ramaswamy,
1358 V., Kahn, R. A., Zhang, P., Dubovik, O., Ding, A., Lacis, A. A., Zhang, L., and Dong,
1359 Y.: Scattering and absorbing aerosols in the climate system, *Nature Reviews Earth and*
1360 *Environment*, 3, 363–379, <https://doi.org/10.1038/s43017-022-00296-7>, 2022.
- 1361 Lilly, D. K.: The representation of small scale turbulence in numerical simulation
1362 experiments, *Proc. Ibm Sci. Comput. Symp. Environ. Sci.*, 320–1951, 195–210, 1967.
- 1363 Lim, K.-S. S., and Hong, S.-Y.: Development of an effective double-moment cloud
1364 microphysics scheme with prognostic cloud condensation nuclei (CCN) for weather
1365 and climate models, *Mon. Wea. Rev.*, 138, 1587–1612,
1366 doi:10.1175/2009MWR2968.1., 2010.
- 1367 Liu, Y., and Daum, P. H.: Parameterization of the autoconversion. Part I: Analytical
1368 formulation of the Kessler-type parameterizations, *J. Atmos. Sci.*, 61, 1539–1548,
1369 doi:10.1175/1520-0469(2004)061,1539:POTAPI.2.0.CO;2, 2004.
- 1370 Lohmann, U., and Diehl, K.: Sensitivity studies of the importance of dust ice nuclei for
1371 the indirect aerosol effect on stratiform mixed-phase clouds, *J. Atmos. Sci.*, 63, 968-
1372 982, 2006.
- 1373 Mansell, E. R., Ziegler, C. L., and Bruning, E. C., Simulated electrification of a small
1374 thunderstorm with two-moment bulk microphysics, *J. Atmos. Sci.*, 67, 171–194,
1375 doi:10.1175/2009JAS2965.1., 2010.
- 1376 Ming, Y., and Chua, X. R.: Convective invigoration traced to warm-rain microphysics,
1377 *Geophys. Res. Lett.*, 47, doi.org/10.1029/2020GL089134, 2020.
- 1378 Mlawer, E. J., Taubman, S. J., Brown, P. D., Iacono, M. J., and Clough, S. A.: RRTM, a
1379 validated correlated-k model for the longwave, *J. Geophys. Res.*, 102, 16663-1668,
1380 1997.
- 1381 Moeng, C.-H., Sullivan, P. P., and Stevens, B.: Including radiative effects in an entrainment
1382 rate formula for buoyancy-driven PBLs, *J. Atmos. Sci.*, 56, 1031 – 1049,
1383 doi:10.1175/1520-0469(1999)056<1031:IREIAE>2.0.CO;2, 1999.
- 1384 Möhler, O., et al, Efficiency of the deposition mode ice nucleation on mineral dustparticles,
1385 *Atmos. Chem. Phys.*, 6, 3007-3021, 2006.
- 1386 Morrison, H., deBoer, G., Feingold, G., Harrington, J., Shupe, M., and Sulia, K., Resilience
1387 of persistent Arctic mixed-phase clouds, *Nat. Geosci.*, 5, 11–17,

- 1388 <https://doi.org/10.1038/ngeo1332>, 2012.
- 1389 Morrison, H., Curry, J. A., and Khvorostyanov, V. I., A new double-moment microphysics
1390 parameterization for application in cloud and climate models. Part I: Description, J.
1391 Atmos. Sci., 62, 1665–1677, 2005.
- 1392 Morrison, H., hompson, G., and V. Tatarskii, Impact of cloud microphysics on the
1393 development of trailing stratiform precipitation in a simulated squall line: Comparison
1394 of one- and two-moment schemes. Mon. Wea. Rev., 137, 991–1007,
1395 <https://doi.org/10.1175/2008MWR2556.1>, 2009.
- 1396 Murakami, M., 1990, Numerical modeling of the dynamical and microphysical evolution
1397 of an isolated convective cloud—The July 19 1981 CCOPE cloud, J. Meteor. Soc.
1398 Japan, 68, 107–128.
- 1399 Ovchinnikov, M., Korolev, A., and Fan, J.: Effects of ice number concentration on
1400 dynamics of a shallow mixed-phase stratiform cloud, J. Geophys. Res., 116, D00T06,
1401 doi:10.1029/2011JD015888, 2011.
- 1402 Possner, A., Ekman, A. M. L., and Lohmann, U.: Cloud response and feedback processes
1403 in stratiform mixed-phase clouds perturbed by ship exhaust, Geophys. Res. Lett., 44,
1404 1964–1972, <https://doi.org/10.1002/2016GL071358>, 2017.
- 1405 Pruppacher, H. R. and Klett, J. D.: Microphysics of clouds and precipitation, 714pp, D.
1406 Reidel, 1978.
- 1407 Ramaswamy, V., et al.: Radiative forcing of climate change, in Climate Change 2001: The
1408 Scientific Basis, edited by J. T. Houghton et al., 349-416, Cambridge Univ. Press,
1409 New York, 2001.
- 1410 [Schima, J., McFarquhar, G., Romatschke, U., Vivekanandan, J., D’Alessandro, J., Haggerty,](#)
1411 [et al.: Characterization of Southern Ocean boundary layer clouds using airborne radar,](#)
1412 [lidar, and in situ cloud data: Results from SOCRATES, J. Geophys. Res., 127,](#)
1413 [e2022JD037277, 2022.](#)
- 1414 Seinfeld, J. H., and Pandis, S. N.: Atmospheric chemistry and physics: From air pollution
1415 to climate change, John Wiley & Sons, 1326 pp, 1998.
- 1416 Solomon, A., de Boer, G., Creamean, J. M., McComiskey, A., Shupe, M. D., Maahn, M.,
1417 and Cox, C.: The relative impact of cloud condensation nuclei and ice nucleating
1418 particle concentrations on phase partitioning in Arctic mixed-phase stratocumulus

Formatted: Font: (Asian) Malgun Gothic, Font color: Black

Formatted: Font: (Asian) Malgun Gothic, Font color: Black

Formatted: Font: (Asian) Malgun Gothic, Font color: Black

Formatted: Font: (Asian) Malgun Gothic, Font color: Black

Formatted: Font: (Asian) Malgun Gothic, Font color: Black

Formatted: Font: (Asian) Malgun Gothic, Font color: Black

Formatted: Font: (Asian) Times New Roman, Italic, Font color: Auto

- 1419 clouds, *Atmos. Chem. Phys.*, 18, 17047–17059, [https://doi.org/10.5194/acp-18-](https://doi.org/10.5194/acp-18-17047-2018)
1420 17047-2018, 2018.
- 1421 Smagorinsky, J.: General circulation experiments with the primitive equations, *Mon. Wea.*
1422 *Rev.*, 91, 99–164, 1963.
- 1423 Stevens, B., et al.: On entrainment rates in nocturnal marine stratocumulus, *Q. J. R.*
1424 *Meteorol. Soc.*, 129, 3469 – 3492, doi:10.1256/qj.02.202, 2003a.
- 1425 Stevens, B., et al.: Dynamics and chemistry of marine stratocumulus-DYCOMS-II, *Bull.*
1426 *Am. Meteorol. Soc.*, 84, 579– 593, doi:10.1175/BAMS-84-5-579, 2003b.
- 1427 Stevens, B., and Feingold, G.: Untangling aerosol effects on clouds and precipitation in a
1428 buffered system, *Nature*, 461, 607–613, <https://doi.org/10.1038/nature08281>, 2009.
- 1429 Stephens, G. L., and Greenwald, T. J.: Observations of the Earth’s radiation budget in
1430 relation to atmospheric hydrology. Part II: Cloud effects and cloud feedback, *J.*
1431 *Geophys. Res.*, 96, 15 325–15 340, 1991.
- 1432 Tinel, C., Testud, J., Hogan, R. J., Protat, A., Delanoe, J. and Bouniol, D.: The retrieval of
1433 ice cloud properties from cloud radar and lidar synergy, *J. Appl. Meteorol.*, 44, 860-
1434 875, 2005.
- 1435 Tsushima, Y., Webb, M. J., Williams, K. D., Soden, B. J., et al.: Importance of the mixed-
1436 phase cloud distribution in the control climate for assessing the response of clouds to
1437 carbon dioxide increase: A multi-model study, *Clim. Dyn.*, 27, 113–126, 2006.
- 1438 Tunved, P., Ström, J. and Krejci, R.: Arctic aerosol life cycle: linking aerosol size
1439 distributions observed between 2000 and 2010 with air mass transport and
1440 precipitation at Zeppelin station, Ny-Ålesund, Svalbard, *Atmos. Chem. Phys.*,
1441 13, 3643–3660, <https://doi.org/10.5194/acp-13-3643-2013>, 2013
- 1442 Twomey, S.: Pollution and the Planetary Albedo, *Atmos. Env.*, 8,1251-1256, 1974.
- 1443 Warren, S. G., Hahn, C. J., London, J., Chervin, R. M., and Jenne, R. L.: Global distribution
1444 of total cloud cover and cloud types over land, NCAR Tech. Note NCAR/TN-
1445 273+STR, National Center for Atmospheric Research, Boulder, CO, 29 pp. + 200
1446 maps, 1986.
- 1447 Wood, R.: Stratocumulus clouds, *Mon. Wea. Rev.*, 140, 2373-2423, 2012.
- 1448 Xue, L., Teller, A., Rasmussen, R. M., Geresdi, I., and Pan, Z.: Effects of aerosol solubility
1449 and regeneration on warm-phase orographic clouds and precipitation simulated by a

1450 detailed bin microphysical scheme, *J. Atmos. Sci.*, 67, 3336–3354, 2010.

1451 Zhang, D., Vogelmann, A., Kollias, P., Luke, E., Yang, F., Lubin, D., and Wang, Z.:
1452 Comparison of Antarctic and Arctic single-layer stratiform mixed-phase cloud
1453 properties using ground-based remote sensing measurements, *J. Geophys. Res.*, 124,
1454 10186–10204, <https://doi.org/10.1029/2019JD030673>, 2019.

1455 Zheng, Y., Zhang, H., Rosenfeld, D., Lee, S. S., Su, T., and Li, Z.: Idealized Large-Eddy
1456 Simulations of Stratocumulus Advecting over Cold Water. Part I: Boundary Layer
1457 Decoupling, 78, 4089-4102, <https://doi.org/10.1175/JAS-D-21-0108.1>, 2021.

1458
1459
1460
1461
1462
1463
1464
1465
1466
1467
1468
1469
1470
1471
1472
1473
1474
1475
1476
1477
1478
1479
1480
1481
1482
1483
1484
1485
1486
1487
1488
1489
1490
1491

1492 **FIGURE CAPTIONS**

1493

1494 Figure 1. A red rectangle marks the simulation domain in the Svalbard area, Norway, and
 1495 a dot in the rectangle marks a ground station which is a part of the Cloudnet observation
 1496 network. The light blue represents the ocean and the green the land area.

1497

1498 Figure 2. (a) The vertical distributions of the domain-averaged potential temperature and
 1499 humidity at the first time step, (b) the time series of the domain-averaged large-scale
 1500 subsidence or downdraft at the model top and (c) the time series of the domain-averaged
 1501 surface temperature.

1502

1503 Figure 3. Aerosol size distribution at the surface. N represents aerosol number
 1504 concentration per unit volume of air and D represents aerosol diameter.

1505

1506 Figure 4. The vertical distributions of the time- and domain-averaged IWC and LWC in
 1507 the 200_2 and 200_0 runs.

1508

1509 Figure 5. The time series of (a) observed and simulated cloud-top and bottom heights, (b)
 1510 retrieved and simulated IWP, and observed and simulated LWP, and (c) the simulated
 1511 surface sensible and latent heat fluxes. Observed and retrieved values are from the ground
 1512 station as marked in Figure 1. For the time series, in the simulation domain, the simulated
 1513 cloud-top height is averaged over grid points with cloud tops and the simulated cloud-
 1514 bottom height is averaged over grid points with cloud bottoms, while the simulated IWP
 1515 and LWP are averaged over grid points with non-zero IWP and LWP, respectively, at each
 1516 time step in the 200_2 run. The simulated surface sensible and latent heat fluxes are
 1517 averaged over the horizontal domain at the surface and each time step in the 200_2 run.

1518

1519 Figure 6. The vertical distributions of the time- and domain-averaged deposition and
 1520 condensation rates in the 200_2 and 200_0 runs.

1521

Deleted: .

1523 Figure 7. The time series of the average supersaturation with respect to ice and water over
1524 grid points where deposition occurs in the presence of both droplets and ice crystals in the
1525 200_2 run.

1526 Figure 8. The vertical distributions of the time- and domain-averaged IWC and LWC in
1527 the 200_2, 200_0 and 200_0.07 runs.

1528

1529 Figure 9. The vertical distributions of the time- and domain-averaged (a) IWC in the 200_2,
1530 2000_20, 200_0.07, 200_20, 2000_2, 2000_0.07, and 200_0.7 runs. (b) The vertical
1531 distributions of the time- and domain-averaged LWC in the 200_0 and 2000_0 runs as well
1532 as all the runs shown in panel (a).

1533

1534 Figure 10. The average size distributions of (a) ice crystals over grid points with non-zero
1535 IWC and the simulation period and (b) drops over grid points with non-zero LWC and the
1536 simulation period.

1537

1538 [Figure 11. IWC/LWC as a function of ICNCavg/CDNCavg based on Table 4.](#)

1539

1540

1541

1542

1543

1544

1545

1546

1547

1548

1549

1550

1551

1552

1553

Deleted: ¶

Simulations	The number concentration of aerosols acting as CCN at the first time step in the PBL (cm^{-3})	The number concentration of aerosols acting as INP at the first time step in the PBL (cm^{-3})	ICNCavg/CDNCavg	Ice processes	Radiation
200 2	200	2	0.220	Present	Present
2000 20	2000	20	0.201	Present	Present
2000 2	2000	2	0.108	Present	Present
200 20	200	20	0.512	Present	Present
200 0	200	2	0.000	Absent	Present
2000 0	2000	2	0.000	Absent	Present
200 0.07	200	0.07	0.022	Present	Present
2000 0.07	2000	0.07	0.012	Present	Present
200 0.7	200	0.7	0.041	Present	Present
4000 45	4000	45	0.220	Present	Present
13 0.1	13	0.1	0.220	Present	Present
4000 1.8	4000	1.8	0.022	Present	Present
12 0.0035	12	0.0035	0.022	Present	Present

1560

1561 Table 1. Summary of simulations

1562

1563

1564

1565

1566

1567

1568

1569

1570

1571

1572

1573

1574

1575

1576

1577

Simulations	IWC (10^3 g m^{-3})	LWC (10^3 g m^{-3})	IWP (g m^{-2})	LWP (g m^{-2})	IWC/LWC	IWP/LWP	Condensation rate		Deposition rate		Cloud-base sedimentation ($10^3 \text{ g m}^{-2} \text{ s}^{-1}$)		Entrainment (cm s^{-1})
							Over grid points (10^2 g m^{-3} s^{-1})	Over cloudy columns (g m^{-2} s^{-1})	Over grid points (10^2 g m^{-3} s^{-1})	Over cloudy columns (g m^{-2} s^{-1})	Ice- crystal	Droplet	
200 2	6.57	0.25	31.94	1.23	26.28	25.96	0.11	1.98	1.30	23.40	1.17	0.17	0.25
2000 20	7.82	0.21	40.91	1.08	37.24	37.91	0.09	1.62	1.57	28.26	0.94	0.06	0.53
2000 2	6.55	0.29	31.85	1.46	22.58	21.81	0.12	2.16	1.28	23.04	1.11	0.08	0.28
200 20	7.80	0.20	40.82	1.01	39.00	40.42	0.09	1.62	1.56	28.08	0.97	0.11	0.51
200 0	0.00	2.06	0.00	10.35	0.00	0.00	0.72	12.48	0.00	0.00	0.00	0.36	0.08
2000 0	0.00	2.25	0.00	11.29	0.00	0.00	0.76	12.80	0.00	0.00	0.00	0.14	0.10
200 0.07	0.89	0.85	4.27	4.20	1.05	1.02	0.32	5.76	0.35	6.30	0.19	0.28	0.06
2000 0.07	0.79	0.97	3.82	4.83	0.81	0.79	0.38	6.84	0.31	5.58	0.17	0.19	0.07
200 0.7	0.98	0.78	4.73	3.88	1.25	1.22	0.31	5.58	0.39	7.02	0.14	0.22	0.07

1578

1579 Table 2. The averaged IWC, LWC, IWP, LWP, condensation and deposition rates over all
1580 of grid points and the simulation period in each of simulations. IWC/LWC (IWP/LWP) is
1581 the averaged IWC (IWP) over the averaged LWC (LWP). Also, as shown are the vertically
1582 integrated condensation and deposition rates over each cloudy column which are averaged
1583 over those columns and the simulation period. The average cloud-base sedimentation rate,
1584 which is for each of ice crystals and droplets, over the cloud base and simulation period,
1585 and the average cloud-top entrainment rate over the cloud top and simulation period are
1586 shown as well.

1587

1588

1589

1590

1591

1592

1593

1594

1595

1596

1597

1598

1599

1600

Simulations	IWC (10^{-3} g m^{-3})	LWC (10^{-3} g m^{-3})	IWP (g m^{-2})	LWP (g m^{-2})	IWC/LWC	IWP/LWP	Condensation rate		Deposition rate		Cloud-base sedimentation ($10^{-3} \text{g m}^{-2} \text{s}^{-1}$)		Entrainment (cm s^{-1})
							Over grid points (10^2 g m^{-3} s^{-1})	Over cloudy columns (g m^{-2} s^{-1})	Over grid points (10^2 g m^{-3} s^{-1})	Over cloudy columns (g m^{-2} s^{-1})	Ice- crystal	Droplet	
200 2 norad	6.42	0.24	31.21	1.22	26.75	25.58	0.10	1.96	1.29	23.35	1.16	0.16	0.24
2000 20 norad	7.63	0.21	40.05	1.07	36.33	37.42	0.09	1.59	1.55	29.91	0.92	0.06	0.51
2000 2 norad	6.40	0.29	31.11	1.45	22.06	21.45	0.11	2.12	1.26	22.69	1.07	0.08	0.27
200 20 norad	7.61	0.20	39.95	0.99	38.05	40.35	0.09	1.59	1.54	27.72	0.97	0.11	0.49
200 0 norad	0.00	2.03	0.00	10.20	0.00	0.00	0.72	12.31	0.00	0.00	0.00	0.34	0.08
2000 0 norad	0.00	2.21	0.00	11.12	0.00	0.00	0.75	12.63	0.00	0.00	0.00	0.13	0.10
200 0.07 norad	0.87	0.84	4.21	4.17	1.04	1.01	0.31	5.74	0.35	6.21	0.18	0.27	0.05
2000 0.07 norad	0.78	0.96	3.78	4.80	0.81	0.79	0.36	6.81	0.30	5.50	0.16	0.18	0.06
200 0.7 norad	0.97	0.76	4.70	3.85	1.25	1.22	0.30	5.55	0.38	6.91	0.13	0.21	0.06

1601

1602 Table 3. Same as Table 2 but for the repeated simulations with radiative processes turned

1603 off.

1604

1605

1606

1607

1608

1609

1610

1611

1612

1613

1614

1615

1616

1617

1618

1619

1620

1621

1622

1623

Simulations	ICNCavg/CDNCavg	Percentage increases (+) or decrease (-) in ICNCavg/CDNCavg	IWC/LWC	Percentage increases (+) or decrease (-) in IWC/LWC
2000 0.07	0.012		0.81	
200 0.07	0.022	+83.33%	1.05	+29.6%
200 0.7	0.041	+86.36%	1.25	+19.0%
2000 2	0.108	+163.4%	22.58	+1706.4%
2000 20	0.201	+86.1%	37.24	+64.9%
200 2	0.220	+9.4%	26.28	-29.4%
200 20	0.512	+132.7%	39.00	+48.4%

1624

1625 Table 4. ICNCavg/CDNCavg and IWC/LWC in the simulations that are related to Section

1626 4.1. The Percentage increases or decreases in ICNCavg/CDNCavg and IWC/LWC as

1627 shown in the i^{th} row are $\frac{(\text{ICNCavg/CDNCavg})_i - (\text{ICNCavg/CDNCavg})_{i-1}}{(\text{ICNCavg/CDNCavg})_{i-1}} \times 100$ (%) and1628 $\frac{(\text{IWC/LWC})_i - (\text{IWC/LWC})_{i-1}}{(\text{IWC/LWC})_{i-1}} \times 100$ (%), respectively. Here, $(\text{ICNCavg/CDNCavg})_i$ and1629 $(\text{IWC/LWC})_i$ represent ICNCavg/CDNCavg and IWC/LWC in the i^{th} row, respectively.

1630

1631

1632

1633

1634

1635

1636

1637

1638

1639

1640

1641

1642

1643

1644

1645

1646

Simulations	ICNCavg/CDNCavg	IWC/LWC	Percentage increases (+) or decrease (-) in IWC/LWC
Polar case			
200_2	0.220	26.28	
4000_45	0.220	27.25	+3.7%
13_0.1	0.220	25.62	-2.5%
Representing midlatitude case			
200_0.07	0.022	1.05	
4000_1.8	0.022	1.09	+3.8%
12_0.0035	0.022	1.02	-2.9%

1647

1648 Table 5. ICNCavg/CDNCavg and IWC/LWC in the simulations that are related to Section

1649 4.2. The percentage increases or decreases in IWC/LWC in the 4000_45 run or in the

1650 13_0.1 run are $\frac{(IWC/LWC)_{4000_45 \text{ or } 13_0.1} - (IWC/LWC)_{200_2}}{(IWC/LWC)_{200_2}} \times 100 (\%)$. Here,1651 $(IWC/LWC)_{4000_45 \text{ or } 13_0.1}$ represents IWC/LWC in the 4000_45 run or the 13_01 run, while1652 $(IWC/LWC)_{200_2}$ represents IWC/LWC in the 200_2 run. The percentage increases or

1653 decreases in IWC/LWC in the 4000_1.8 run or the 12_0.0035 run are

1654 $\frac{(IWC/LWC)_{4000_1.8 \text{ fac10 or } 12_0.0035 \text{ fac10}} - (IWC/LWC)_{200_2 \text{ fac10}}}{(IWC/LWC)_{200_2 \text{ fac10}}} \times 100 (\%)$. Here,1655 $(IWC/LWC)_{4000_1.8 \text{ or } 12_0.0035}$ represents IWC/LWC in the 4000_1.8 run or the 12_0.00351656 run, while $(IWC/LWC)_{200_0.07}$ represents IWC/LWC in the 200_0.07 run.

1657

1658

1659

1660

1661

1662

1663

1664

1665

1666

1667

1668

1669

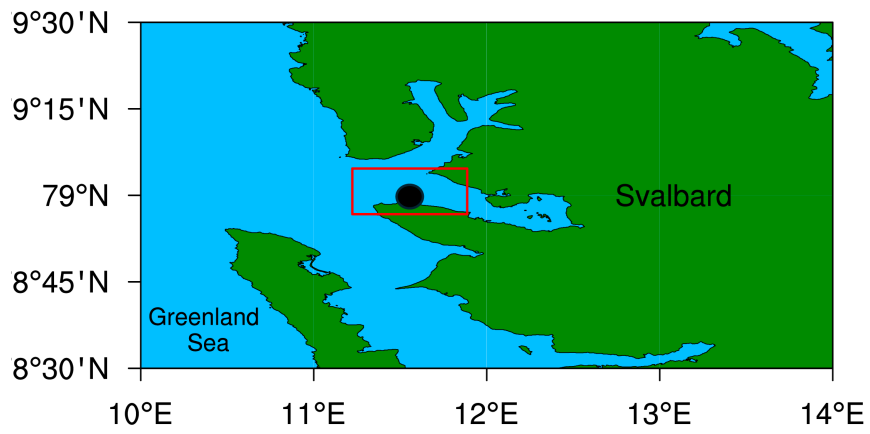
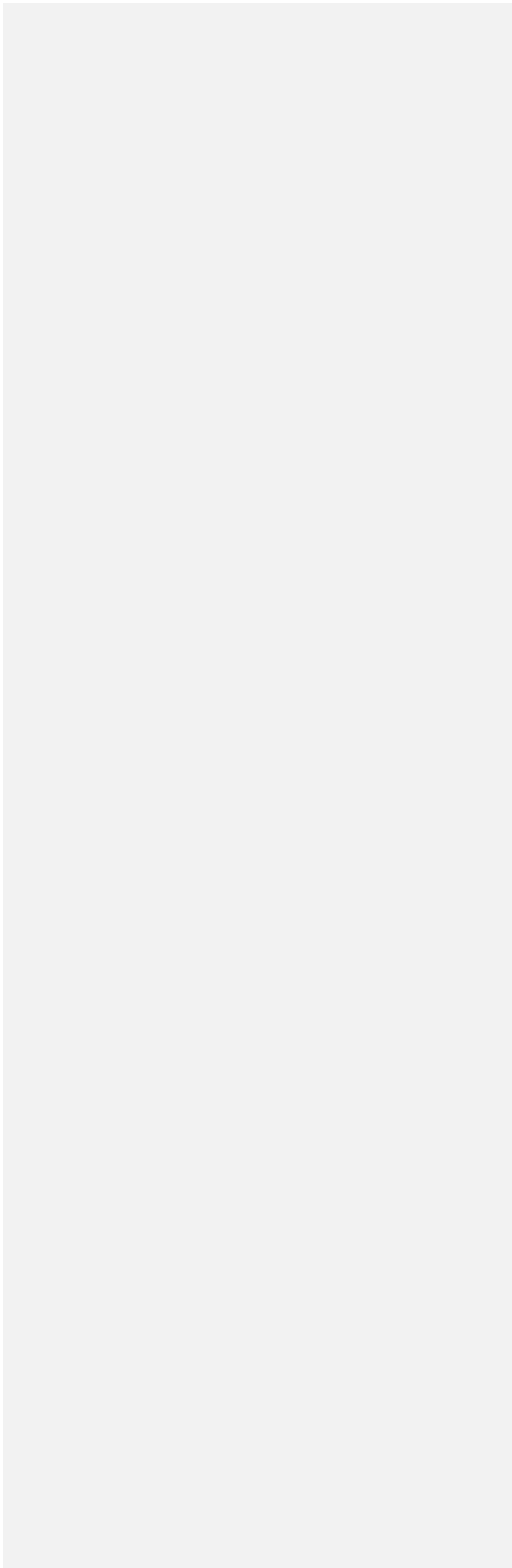
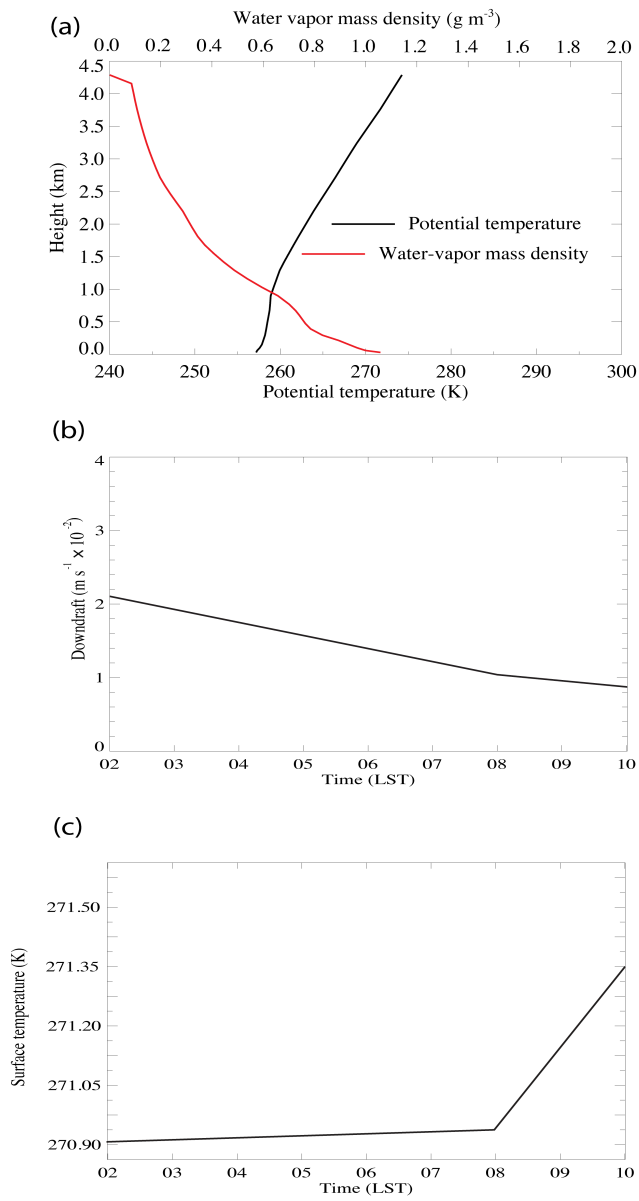


Figure 1

1670
1671
1672
1673
1674
1675
1676
1677
1678
1679
1680
1681
1682
1683
1684
1685
1686
1687
1688
1689

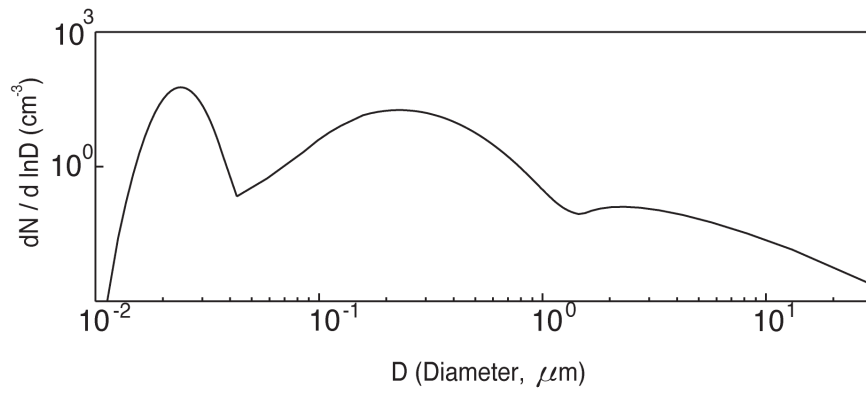




1690

1691

Figure 2

**Figure 3**

1692

1693

1694

1695

1696

1697

1698

1699

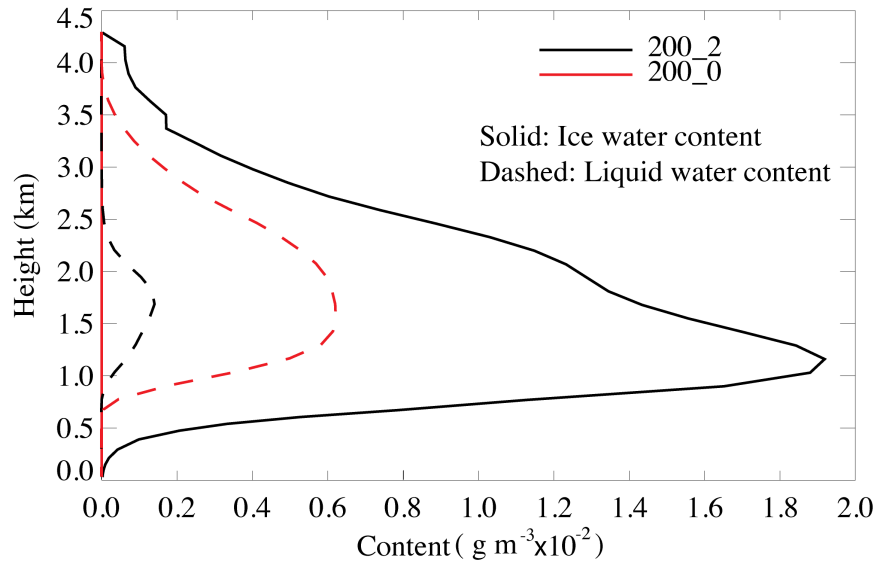
1700

1701

1702

1703

1704



1705

1706

1707

1708

1709

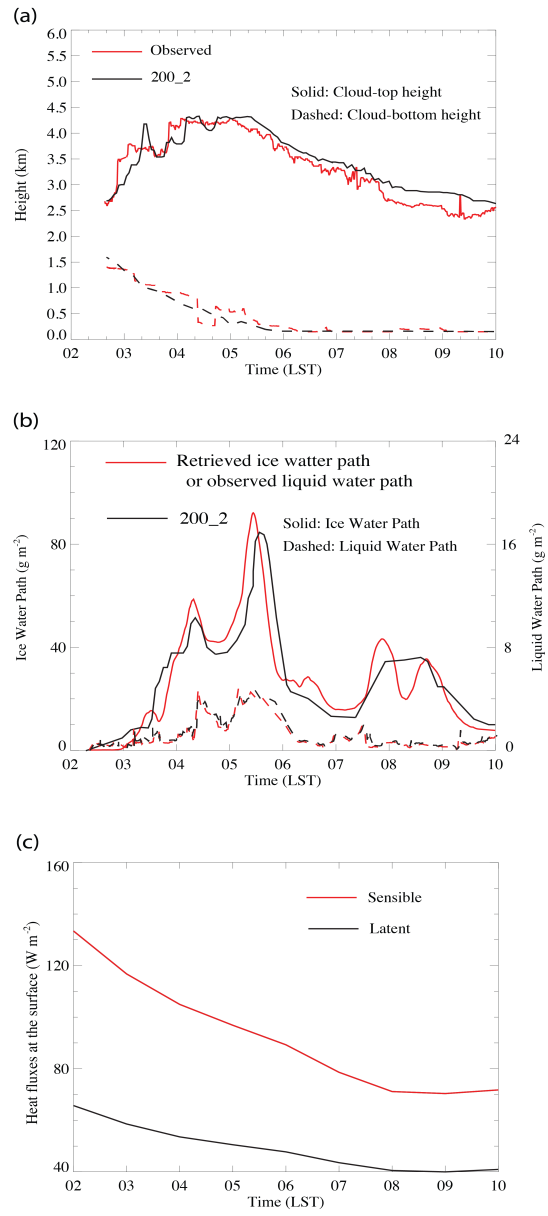
1710

1711

1712

1713

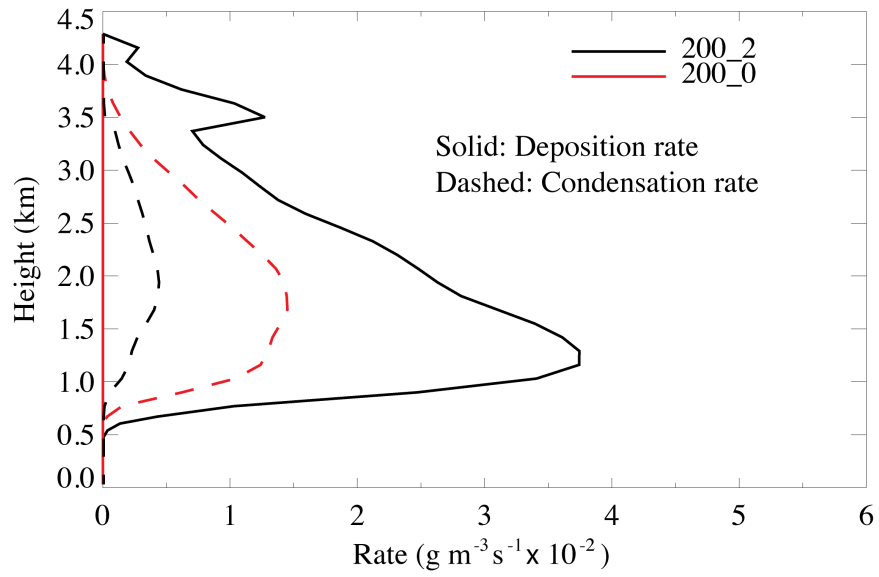
Figure 4



1714

1715

Figure 5

**Figure 6**

1716

1717

1718

1719

1720

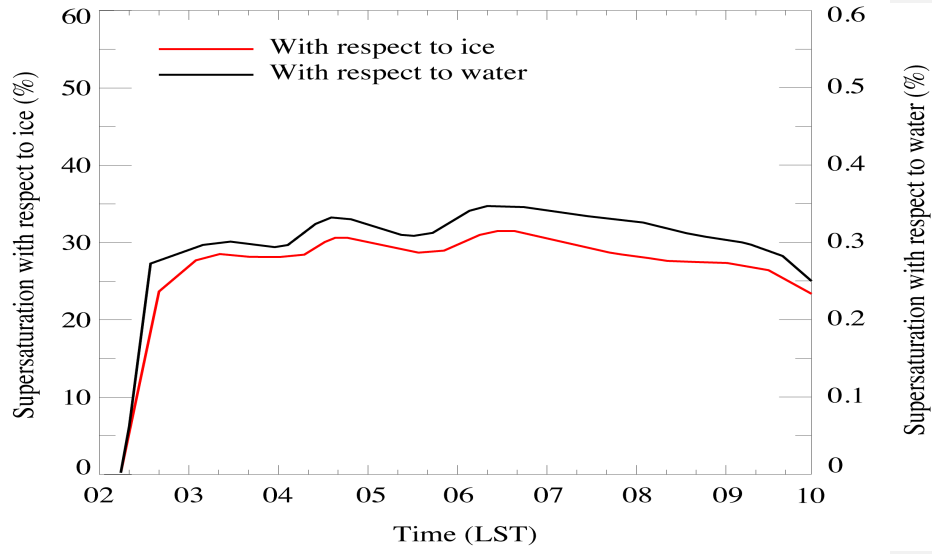
1721

1722

1723

1724

1725

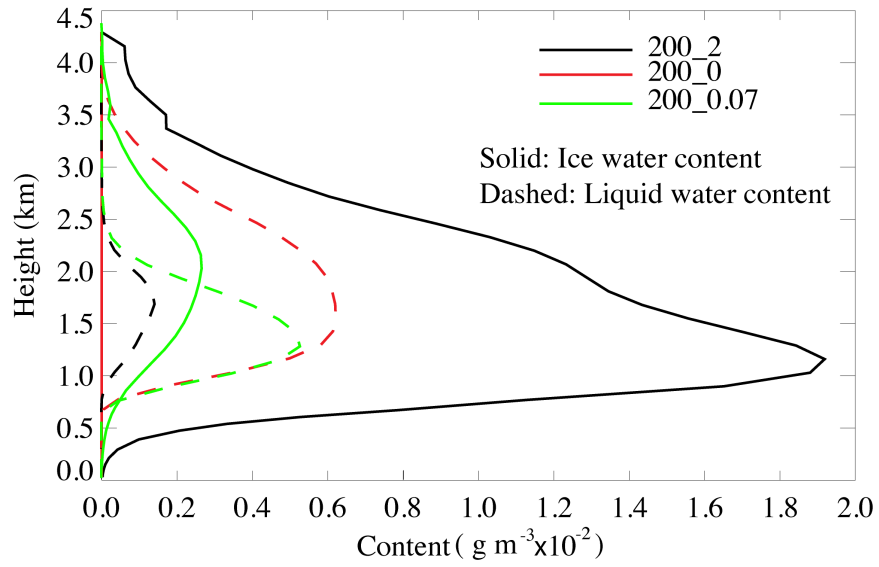


1726

1727

1728

Figure 7



1729

1730

Figure 8

1731

1732

1733

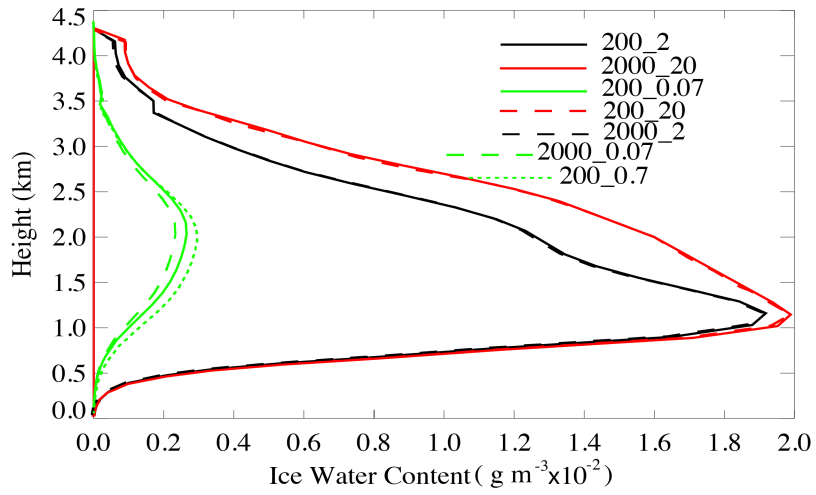
1734

1735

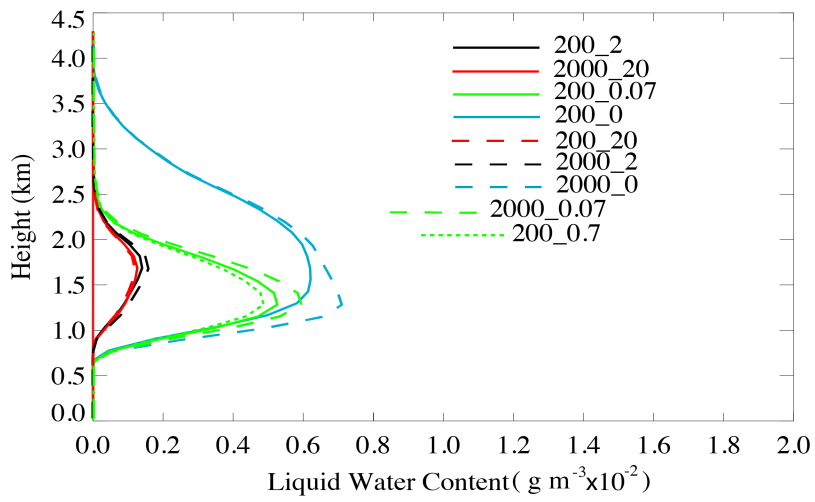
1736

1737

(a)



(b)



1738

1739

Figure 9

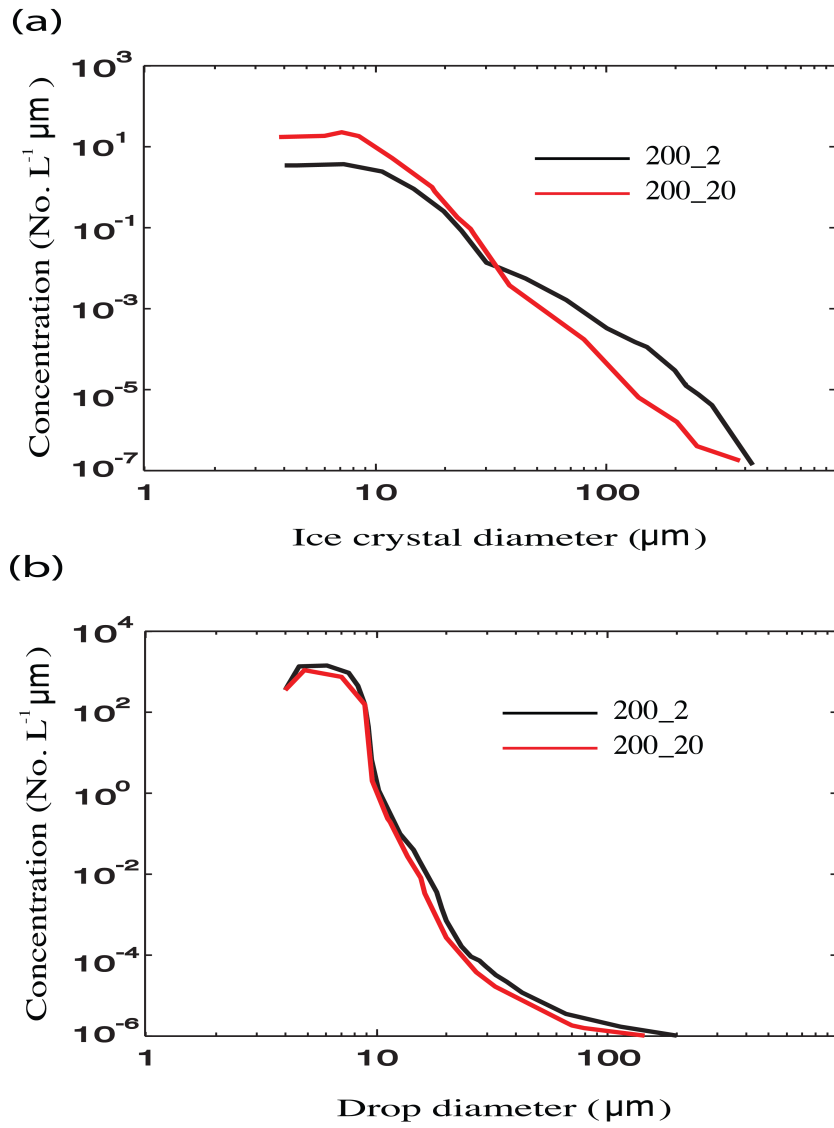
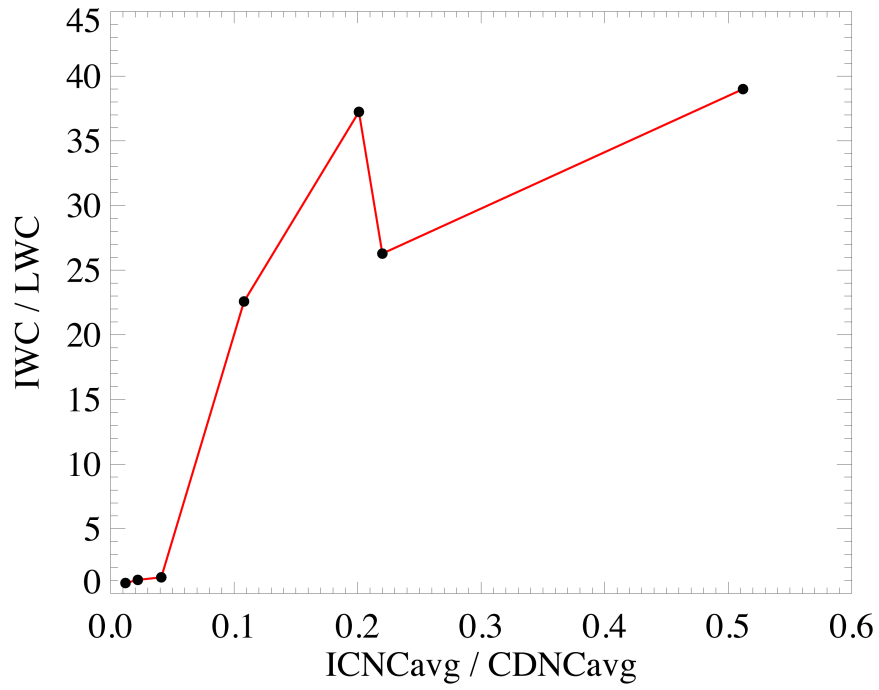


Figure 10



1742

1743

1744

Figure 11